Fisheries and Oceans Canada | Pêches et Océans Canada
Ecosystems and Oceans Science | Sciences des écosystèmes et des océans

Canadian Science Advisory Secretariat (CSAS)

Research Document 2025/082

National Capital Region

American Eel (*Anguilla rostrata*) Freshwater Population Trajectory in Canada

Adam S. van der Lee and Marten A. Koops

Fisheries and Oceans Canada
Great Lakes Laboratory for Fisheries and Aquatic Sciences
867 Lakeshore Rd.
Burlington, ON L7S 1A1

December 2025

Canada

Foreword

This series documents the scientific basis for the evaluation of aquatic resources and ecosystems in Canada. As such, it addresses the issues of the day in the time frames required and the documents it contains are not intended as definitive statements on the subjects addressed but rather as progress reports on ongoing investigations.

Published by:

Fisheries and Oceans Canada
Canadian Science Advisory Secretariat
200 Kent Street
Ottawa ON K1A 0E6

http://www.dfo-mpo.gc.ca/csas-sccs/
DFO.CSAS-SCAS.MPO@dfo-mpo.gc.ca

ISSN 1919-5044
ISBN 978-0-660-79921-6 Cat. No. Fs70-5/2025-082E-PDF

Correct citation for this publication:

van der Lee, A.S. and Koops, M.A. 2025. American Eel (*Anguilla rostrata*) Freshwater Population Trajectory in Canada. DFO Can. Sci. Advis. Sec. Res. Doc. 2025/082. iv + 56 p.

Aussi disponible en français :

*van der Lee, A.S., et Koops, M.A. 2025. Trajectoire de la population d'anguilles d'Amérique (*Anguilla rostrata*) en eau douce au Canada. Secr. can. des avis sci. du MPO. Doc. de rech. 2025/082. iv + 62 p.*

TABLE OF CONTENTS

ABSTRACT

Describing trends in American Eel (*Anguilla rostrata*) abundances has been tackled regularly at various locations across its range; however, describing a common trajectory for the whole panmictic population has been a challenge. As a step toward this broader challenge, 12 fishery-independent datasets from freshwater across the Canadian range were used to estimate a Canada-wide trajectory of American Eel relative abundance. These datasets averaged 29 years per time series (range: 14-65) over the 1952-2018 time period. Time series mostly tracked yellow eel (n = 10), with some elver (n = 1) and silver eel (n = 1). Each dataset was standardized to control for potentially confounding factors, and the standardized statistical models were used to generate a standardized time series of relative abundance. These standardized relative abundances were transformed to a common scale, and a Canada-wide trend was fit. Generally, datasets with more historical data had more negative year trends. The Canada-wide trend produced mean rates of decline of -0.021 to -0.046 per year since 1980. The model indicated a 100% likelihood that the Canadian freshwater population has declined since 1980 and a 69.2-100% likelihood that the decline was greater than 50%. Limiting data to the 2000-2018 years produced less negative trends that generally did not differ from zero. Results were robust to the data standardizations, inclusion or exclusion of individual datasets, and adjustments for the spatial distribution of data. Overall, this analysis shows that while American Eel freshwater abundance in Canada has been stable over the last two decades, significant declines preceded this time period and were not limited to the St. Lawrence basin.

INTRODUCTION

American Eel (*Anguilla rostrata*) occupy an extensive range throughout the entire western North Atlantic coastline, extending from the north coast of South America to Greenland (Figure 1). American Eel occupy freshwater, brackish and coastal marine habitats, exhibiting a unique life-history strategy where semelparous adults, called silver eel, undertake extensive migrations to the Sargasso Sea to spawn as a single panmictic breeding population. The larvae, called leptocephali, are distributed along the western North Atlantic coastline. After reaching the coastline, leptocephali transition into glass eels and then elvers. As they grow and become more pigmented, they are referred to as yellow eel, which represent an extended juvenile stage. Finally, they mature and develop into silver eel, migrate to the Sargasso Sea, spawn, and die.

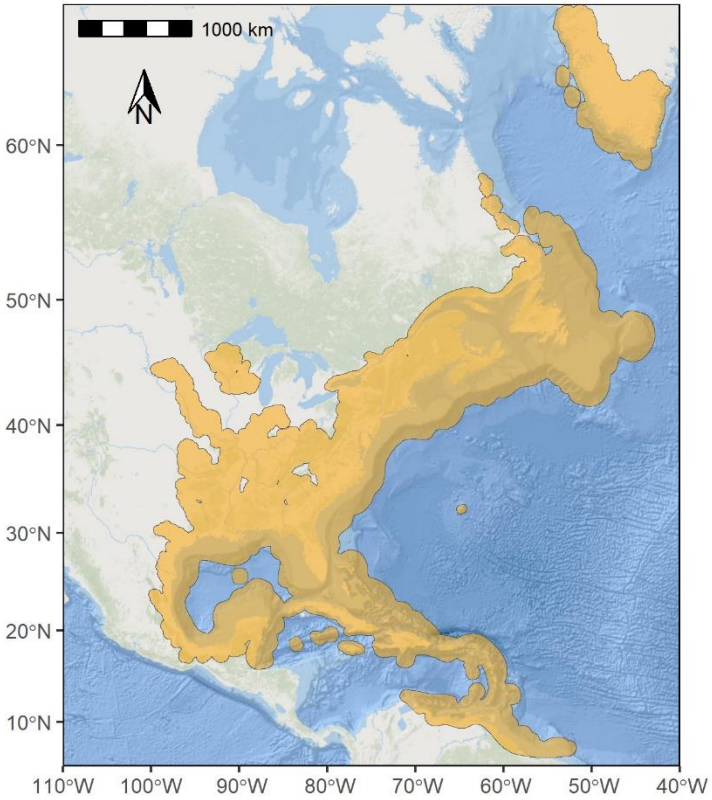

Figure 1. American Eel distribution. Data from IUCN redlist website for American Eel (ASSG 2014, IUCN 2022).

In Canada, American Eel occupy all habitats accessible from the Atlantic Ocean, throughout the Maritimes to the Labrador coast and up the St. Lawrence River to Lake Ontario (Figure 2). The distribution of American Eel has been divided into zones based on watershed boundaries (DFO 2014). Five zones were identified in Canada: Scotia Fundy, Southern Gulf of St. Lawrence, Northern Gulf of St. Lawrence, the St. Lawrence Basin, and Labrador (Figure 1). Within each of these zones are numerous tributaries occupied by American Eel. There is no evidence of genetic differentiation among sub-populations and the species, as a whole, is considered one population (Côte et al. 2013). Understanding and describing the trajectory of this panmictic population has been a challenge.

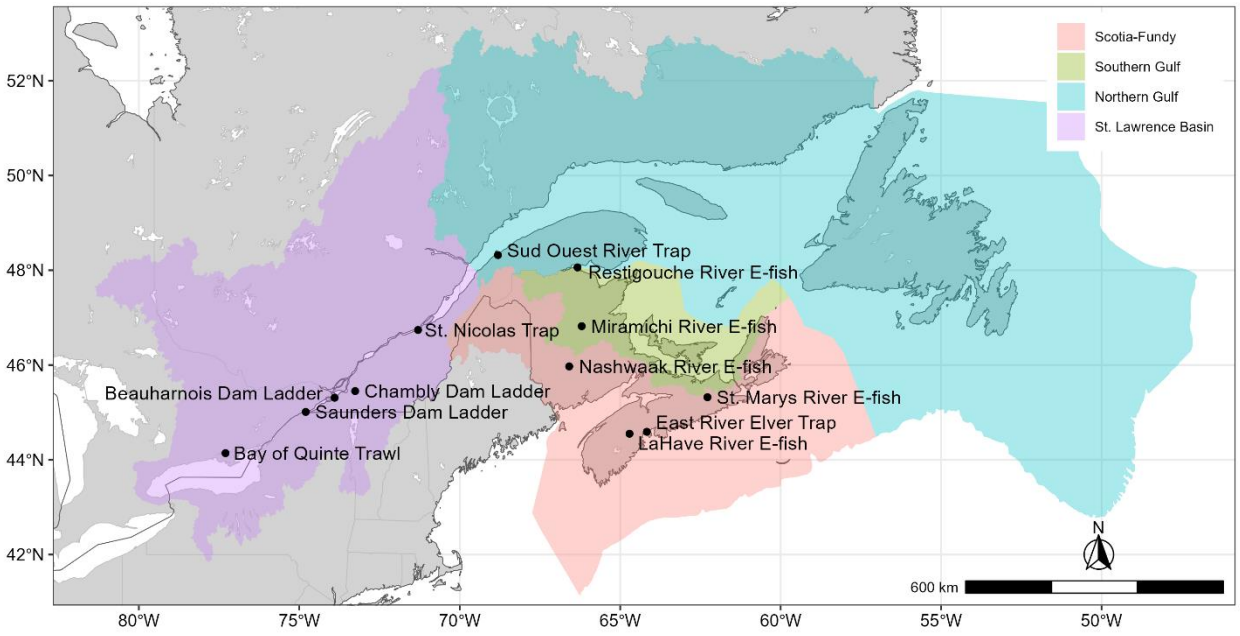

Figure 2. Canadian distribution of American Eel divided into zones (colours). Dataset location are indicated. Data from Cairns et al. (2014) and Cairns (2020).

Describing and analysing the trend in American Eel abundance has been tackled regularly over the past few decades. However, these analyses typically rely on single indicators (e.g., Drouineau et al. 2018), focus on one or a few closely related locations (e.g., Greer 2003), or describe the trends across multiple widely dispersed locations (e.g., Haro et al. 2000).

Range-wide, the International Union for Conservation of Nature (IUCN) assessed the American Eel as Endangered (Jacoby et al 2017). Within Canada, American Eel was assessed by the Committee on the Status of Endangered Wildlife in Canada, as a single designatable unit (DU), as Threatened (COSEWIC 2012). This designation was driven by significant declines in portions of its distribution (St. Lawrence Basin zone) and extensive threats from dams and pollution. Dams create barriers restricting access to large areas of habitat for migrating juveniles and significant mortality can occur on out migrating silver eels from hydroelectric turbine strikes (> 40%) (Verreault and Dumont 2003). The status report noted that trends in relative abundance across zones were variable. Bowlby (2018) provided an analysis of three rivers in Nova Scotia, showing declines of 44% (LaHave River, 1995-2017), 88% (Shubenacadie River, 1995-2005), and 91% (St. Mary's River, 1995-2017). Cornic et al. (2021) examined Canadian abundance indices, and for 12 fishery-independent data sets concluded that six were stable, four showed declines, and 2 exhibited increases. However, no attempt was made to synthesize these analyses into a Canada-wide trend analysis. Consequently, the trajectory of the abundance of American Eel in Canada as a whole is not clear. As a panmictic population, subject to regional regulations and protections, it is important to discern how the entire population is performing as the various zones are unlikely to be independent of each other.

To date, only ASMFC (2017, 2023) and Kahn (2019) have provided synthetic American Eel abundance trends over broad areas of the U.S. Atlantic coast. By creating indices of relative abundance based on fishery-independent surveys (ASMFC 2017, 2023) or recreational catch and effort data (Kahn 2019), which showed that American Eel abundance declined through to the mid-1990s, then held stable until the early 2000s. The ASMFC (2017) index shows

continuation of stable relative abundances through to 2016, while the Kahn (2019) index shows some more recent increases.

The objective in this report, is to analyse and synthesise the available long-term, fisheries-independent time series of American Eel abundances, building on previous work (Cornic et al. 2021, Cairns 2020), to generate an estimate of the Canada-wide trajectory of relative abundance in freshwater. This will provide a clearer picture of the status of American Eel in Canada.

METHODS

DATA

Twelve long-term, fisheries independent datasets have been identified as time series that could provide insight into the changes of relative eel abundance and inform population trajectory (Cairns 2020, Figure 2). These datasets were previously analysed by Cornic et al. (2021). Four of the five Canadian zones are represented with four datasets from within the Scotia Fundy zone, two from the Southern Gulf zone, one from the Northern Gulf zone, five from the St. Lawrence Basin Zone, and no dataset from within the Labrador zone. All time series were from freshwater locations. There are significant differences among the datasets in how eel were sampled, which life-stage(s) were targeted and the length of the time series (Table 1, Figure 3). See Cairns (2020) for a detailed description of each dataset.

Table 1. Summary of datasets analysed.

Zone	Location	Gear	Stage	Years	N
Scotia Fundy	LaHave River, NS	backpack electrofisher	yellow eel	1995, 1996, 1998-2017	251
	Nashwaak River, NB	backpack electrofisher	yellow eel	1988-2018	395
	St. Marys River, NS	backpack electrofisher	yellow eel	1995-2017	290
	East River, Chester, NS	elver trap	elver	1996-2002, 2008-2018	1,138
Southern Gulf	Miramichi River, NB	backpack electrofisher	yellow eel	1952-1990, 1992-2018	2,978
	Restigouche River, NB	backpack electrofisher	yellow eel	1972-1983, 1985-1991, 1992, 1994, 1998-2018	2,184
Northern Gulf	Sud-Ouest River, QC	fishway trap	yellow eel	1999-2001, 2003-2016	1,036
St. Lawrence Basin	Bay of Quinte, ON	bottom trawl	yellow eel	1972-1988, 1990-2017	1,540
	Moses-Saunders Dam, ON	eel ladder trap	yellow eel	1979-1995, 2006-2016, 2018	1,537 & 1,394
	Beauharnois, Dam, QC	eel ladder trap	yellow eel	2002-2018	1,741
	Chambly Dam, QC	eel ladder trap	yellow eel	2004-2018	1,475
	Saint-Nicolas trap, St. Lawrence River, QC	estuary trap	silver eel	1975-2014, 2017-2018	4,726

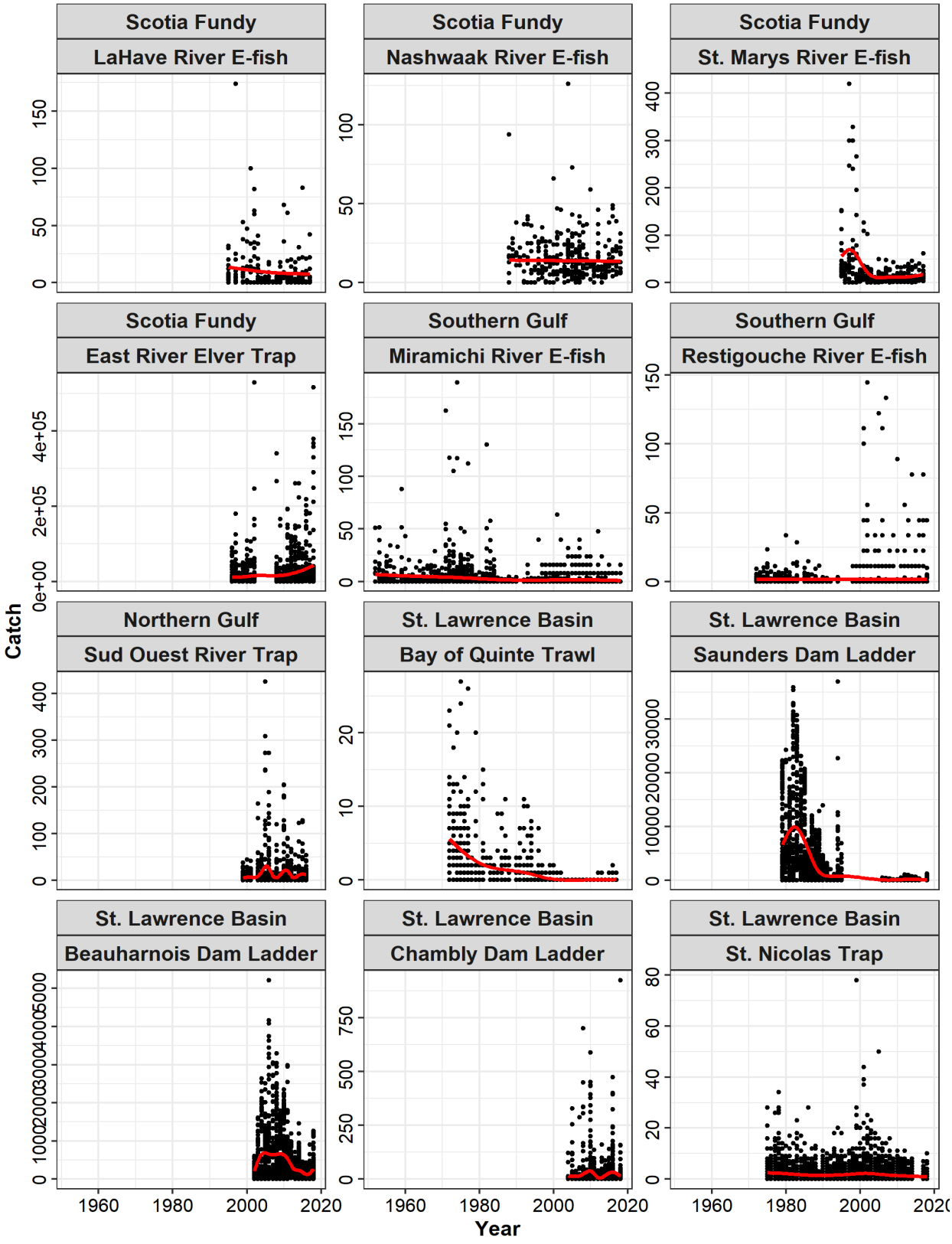

Figure 3. Eel catch data plotted against sample year for each dataset with zone indicated. The red line is a smoothed trend line fit as a cubic spline.

MODELS

To estimate a Canada-wide trajectory of relative abundance from these twelve datasets (Table 1, Figure 3), the following steps were applied to the analysis. First, each individual time series was standardized. Due to factors such as changes in sampling effort, timing, environmental conditions, etc. that occur throughout a monitoring program the ability to detect and catch American Eel may vary among and within years. The standardization of each time series aims to control for potential confounding factors so that relative abundance can be compared through time. Second, annual estimates of relative abundance were extracted based on the 'best' standardization model for each dataset from the suite of alternative model structures explored. This provided a standardized time series of relative abundance for each dataset. Third, the standardized relative abundance indices were transformed to a common scale for comparison. Despite standardization, the time series remained on vastly different scales (e.g. catch-per-unit-effort from electrofishing or daily eel counts from an eel ladder). Fourth, the Canada-wide trend was modelled based on the transformed relative abundance indices using generalized linear mixed models (GLMM) and dynamic factor analysis (DFA). The GLMM analysis was performed on standardized and raw abundance indices and separate analyses included all data series (n = 12), as well as, only those targeting the yellow eel stage (n = 10). Finally, a number of checks were performed on the influence of the data standardization, individual datasets, and uneven zone representation on the estimated Canada-wide trajectory.

Standardization models

All standardization models were constructed as generalized linear mixed models (GLMM) and fit using INLA (Integrated Nested Laplace Approximation; Rue et al. 2009). INLA is a method for making fast and accurate Bayesian approximations and provides greater flexibility in model formation than many frequentist methods and quicker model fitting than Markov Chain Monte Carlo methods.

The standardization models for each dataset were constructed similarly. All datasets had eel count as a response variable, therefore, each GLMM utilized a probability distribution capable of handling positive integers and applied the logarithmic link function ($\log_e$). Each model incorporated an intercept, α, and $year$ as the first fixed effect, with $year$ centred before inclusion in the model. With the logarithmic link function the slope of $year$ represents r in the exponential model of population growth ($N_t = N_0 e^{rt}$) with e^{α} representing N_0. Additional fixed effects covariates were incorporated but varied among datasets depending on data availability and dataset-specific considerations (i.e., factors that may influence specific sampling methods or life-stage sampled). All covariates were centred and scaled before inclusion in the model. The inclusion of random effects, z_j, to account for site effects or sub-annual temporal effects was explored. Finally, an inter-annual temporal random effect was included in each standardization model, v_t, which accounts for variability around the $year$ trend and was important for deriving predictions from the standardization models. All standardization models utilized the following model structure:

$$\log_e(\mu_{ijt}) = \alpha + \beta_1 \cdot year + \beta_{2\ldots n} \cdot covariates_{2\ldots n} + z_j + v_t. \quad (1)$$

The random effect, z_j, were either assumed to be independently and identically distributed (iid) where $e_j \sim N(0, \sigma_j^2)$ if a simple random intercept structure was desired (e.g., to account for a site effect) or a random walk order 2 (rw2) structure was assumed, where:

$$z_j = (2 \cdot z_{j-1} - z_{j-2}) + e_j \ \ where\ e_j \sim N(0, \sigma_j^2), \quad (2)$$

to account for sub-annual temporal trends (e.g., a daily, weekly, or monthly trend). The inter-annual temporal random effect was modelled using an autoregression order 1 (ar1) structure, where:

$$v_t = \rho \cdot v_{t-1} + e_t \; where \; e_t \sim N(0, \sigma_t^2), \quad (3)$$

where ρ is the correlation among years.

For each standardization model a variety of probability distributions and random effect structures were explored. The probability distributions explored were Poisson, Negative Binomial (NB), Tweedie, Zero-inflated Poisson (ZIP), and Zero-inflated Negative Binomial (ZINB) (Table 2). Each of these distributions are applicable to positive discrete data; the NB, Tweedie, and ZINB have additional parameters that allow for over-dispersion relative to the Poisson distribution; the Tweedie, ZIP, ZINB have an additional point mass at zero to allow for an excess in the number of zero observations present in the dataset. In INLA, it is not possible to explicitly model the "false zeros" portion of the ZIP or ZINB distribution with additional covariates.

Table 2. Parameterization of prospective probability distributions used in standardization models.

Distribution	Parameterization	Definition
Poisson	$y_i \sim Poisson(\mu_i)$ $E(y_i) = \mu_i$ $var(y_i) = \mu_i$	μ_i = mean
Negative Binomial	$y_i \sim NB(\mu_i, \mathrm{k})$ $E(y_i) = \mu_i$ $var(y_i) = \mu_i + \frac{{\mu_i}^2}{\mathrm{k}}$	μ_i = mean k = size
Tweedie	$y_i \sim Tweedie(\mu_i, p, \phi)$ $E(y_i) = \mu_i$ $var(y_i) = \phi \cdot {\mu_i}^p$	μ_i = mean p = Tweedie power parameter ϕ = dispersion parameter
Zero-inflated Poisson	$y_i \sim ZIP(\mu_i, \pi)$ $E(y_i) = (1-\pi) \cdot \mu_i$ $var(y_i) = (1-\pi) \cdot (\mu_i + \pi \times {\mu_i}^2)$	μ_i = mean π = proportional zero inflation
Zero-inflated Negative Binomial	$y_i \sim ZINB(\mu_i, \pi, \mathrm{k})$ $E(y_i) = (1-\pi) \cdot \mu_i$ $var(y_i) = (1-\pi) \cdot \mu_i \cdot (1 + \pi \cdot \mu_i + \frac{\mu_i}{k})$	μ_i = mean π = proportional zero inflation k = size

Models were fit with the full suite of potential fixed effects with varying probability distributions and random effects structures. The fits of the resultant models were compared with a variety of methods with the 'best' model selected. The methods used to assess model fit include Bayesian p-values of fit statistics, DHARMa residuals (Harting 2022), and Watanabe-Akaike information criterion (WAIC, Watanabe 2010).

Bayesian p-values compare the proportion of fit statistics estimated from simulated data generated from the model that exceed the fit statistic estimated from the observed data. Values close to 0.5 indicate good fit. Three fit statistics were used: sum of squared estimates (SSE), where:

$$SSE = \sum \left[\frac{y_i - E(y_i)}{{\sigma_y}^2} \right]^2, \quad (4)$$

Residual variance, where:

$$residual\ variance = var(y_i - E(y_i)), \quad (5)$$

and the proportion of zeros, where the number of observed zeros was compared to those generated across simulations.

DHARMa residuals use a simulation-base approach to generate interpretable residuals for GLMMs. The residuals are scaled between 0 and 1 and describe the proportion of simulated data points above or below the observed value. The residuals should follow a uniform distribution, assessed with a Kolmogorov-Smirnov test, with no obvious trend when plotted against the rank order transformed fitted values, assessed visually.

Once the 'best' model was selected, giving the preferred probability distribution and random effect structure, a step-wise procedure was used to reduce the fixed effects based on parameter significance and ΔWAIC, covariates were remove when they had a non-significant parameter and its removal did not worsen WAIC by more than two.

For all random effect standard deviation parameters (σ_j and σ_t) penalised complexity priors were used (Simpson et al. 2017), with a u parameter of three times the standard deviation of y with respect to the potential random effect (with a maximum value of 5) and $\alpha = 0.01$; specifying that there is a 1% probability of the random effect σ being greater than three times the standard deviation. Penalised complexity priors were also used for the autocorrelation parameter of the AR1 temporal trend, assuming $\rho = 1$ as the base model (Sorbye and Rue 2017) with u and α parameters of 0 and 0.9; indicating a 90% probability that $\rho > 0$.

Scotia Fundy

LaHave River Electrofishing

The LaHave River dataset comes from a single pass electrofishing survey where the primary goal is to monitor Atlantic Salmon (*Salmo salar*) abundance. Data were available from 1995 to 2017 but with sampling not taking place in 1996 and 1998. The dataset was limited to sites that were sampled in at least two years. Eel count per sample was used as the response variable. Potential covariates included temperature, flow ($\log_e$-transformed to reduce the impact of large values), month (July, August, September), and positional data (longitude and latitude). Sampling effort varied among samples therefore $\log_e$(Area sampled) was used as an offset.

Indicators of sample site and tributary were included in the dataset which could represent potential grouping factors for inclusion as random effects. The model structures explored included: no additional random effects ($z_j = 0$), site as a random effect ($z_j = site_j$), tributary as a random effect $z_j = tributary_j$, and site and tributary as random effects $z_{jk} = site_j + tributary_k$. The random effects were assumed to follow an iid structure.

Nashwaak River Electrofishing

The Nashwaak River dataset is also from the Atlantic Salmon electrofishing monitoring survey. Data were available from 1988 to 2018. The dataset was limited to sites that were sampled in at least two years and sampled in months: July, August, and September (only seven and five samples occurred in June and October respectively). Eel count per sample was used as the response variable. Potential covariates included temperature, flow ($\log_e$-transformed to reduce the impact of large values), month (July, August, September), and positional data (longitude and latitude). Sampling effort varied among samples therefore $\log_e$(Area sampled) was used as an offset.

An indicator of sample site was included in the dataset which could represent a potential grouping factor for inclusion as a random effect. The model structures explored included: no

additional random effects ($z_j = 0$) and site as a random effect ($z_j = site_j$). The random effects were assumed to follow an iid structure.

St. Marys River Electrofishing

The St. Marys River dataset is also from the Atlantic Salmon electrofishing monitoring survey. Data were available from 1995 to 2017. The dataset was limited to sites that were sampled in at least two years. Eel count per sample was used as the response variable. Potential covariates included temperature, flow ($\log_e$-transformed to reduce the impact of large values), month (July, August, September), and positional data (longitude and latitude). Sampling effort varied among samples therefore $\log_e$(Area sampled) was used as an offset.

Indicators of sample site and tributary were included in the dataset which could represent potential grouping factors for inclusion as random effects. The model structures explored included: no additional random effects ($z_j = 0$), site as a random effect ($z_j = site_j$), tributary as a random effect $z_j = tributary_j$, and site and tributary as random effects $z_{jk} = site_j + tributary_k$. The random effects were assumed to follow an iid structure.

East River Elver Trap

The East River dataset is from an elver monitoring program from southwestern Nova Scotia using four “Irish style” collection traps (Bradford et al. 2022). Daily elver counts were made from volumetric estimation. Data were limited to months April to July. Data were available from 1996 to 2002 and from 2008 to 2018. Despite the time gap the data were incorporated into a single model. Potential covariates include month, temperature, tide and lunar phase.

Sub-annual temporal trends were included as potential random effects, using an rw2 structure, to account for variation in catch within a year. The various random effect structures explored were: no additional random effects ($z_j = 0$), month as a random effect ($z_j = month_j$), week as a random effect ($z_j = week_j$) and day of the year as a random effect ($z_j = day_j$); in addition, fits were made with the month or week random effects being allowed to varying among years ($z_{jt} = month_{jt}$ or $z_{jt} = week_{jt}$), which allows the intra-annual trend to be different each year. A year-varying day random effect was not fit as the number of random effects would exceed the number of data points. When sub-annual temporal trends were included in the model fit month was not included as a fixed effect.

Southern Gulf

Miramichi River Electrofishing

The Miramichi River dataset comes from an electrofishing survey targeting Atlantic Salmon, which historically included five-pass depletions sampling but has used mostly single-pass methods since 1993. Catchability-corrected eel counts from the first pass were used as the response variable. Data were available from 1952-2018 except for 1991. Potential covariates included temperature, flow ($\log_e$-transformed to reduce the impact of large values), month (June to October), and positional data (longitude and latitude). Sampling effort varied among samples therefore $\log_e$(Area sampled) was used as an offset.

An indicator of sample site was included in the dataset which could represent a potential grouping factor for inclusion as a random effect. The model structures explored included: no additional random effects ($z_j = 0$) and site as a random effect ($z_j = site_j$). The random effects were assumed to follow an iid structure.

Restigouche River Electrofishing

The Restigouche River dataset was from a similar electrofishing survey targeting Atlantic Salmon. Catchability-corrected eel counts from the first pass were used as the response variable. Data were available from 1972 to 2018, with the years 1984, 1993, and 1995-1997 missing. Potential covariates included temperature, flow ($\log_e$-transformed to reduce the impact of large values), and month (June to October). Sampling effort varied among samples therefore $\log_e$(Area sampled) was used as an offset.

An indicator of sample site was included in the dataset which could represent a potential grouping factor for inclusion as a random effect. The model structures explored included: no additional random effects ($z_j = 0$) and site as a random effect ($z_j = site_j$). The random effects were assumed to follow an iid structure.

Northern Gulf

Sud Ouest River Trap

The Sud Ouest River dataset is from an American Eel monitoring survey where eel were counted in a trap at the top of a fishway above a 15 m high waterfall. Daily trap counts were used as the response variable. Data were available from 1999 to 2016, except for 2002. Data were limited to months June, July, and August which were consistently sample throughout the timeseries. Potential covariates included temperature as, up to, a second degree polynomial, flow ($\log_e$-transformed to reduce the impact of large values), month, and lunar phase.

Sub-annual temporal trends were included as potential random effects, using an rw2 structure, to account for variation in catch within a year. The various random effect structures explored were: no additional random effects ($z_j = 0$), month as a random effect ($z_j = month_j$), week as a random effect ($z_j = week_j$) and day of the year as a random effect ($z_j = day_j$); in addition, fits were made with the month or week random effect being allowed to varying among years ($z_{jt} = month_{jt}$ or $z_{jt} = week_{jt}$), which allows the intra-annual trend to be different each year. A year-varying day random effect was not fit as the number of random effects would exceed the number of data points. When sub-annual temporal trends were included in the model fit month was not included as a fixed effect.

St. Lawrence Basin

Bay of Quinte Trawl

The Bay of Quinte dataset comes from a long-term bottom trawl survey conducted to monitor the broader fish community. Five sites were consistently monitored throughout the time series at a similar depth range and were maintained in the analysis (two sites BQ16 and BQ17 were excluded). The data were limited to consistently sampled months (May to October). Eel count per trawl was used as the response variable. Effort was consistent among trawls with trawls lasting six minutes and sampled an area of 0.24 ha. Potential covariates included temperature, flow ($\log_e$-transformed to reduce the impact of large values), and month.

An indicator of sample site was included in the dataset which could represent a potential grouping factor for inclusion as a random effect. The model structures explored included: no additional random effects ($z_j = 0$) and site as a random effect ($z_j = site_j$). The random effects were assumed to follow an iid structure.

Moses-Saunder Eel Ladder

The Moses-Saunders Dam is located on the St. Lawrence River near Cornwall, ON. An eel ladder was installed on the Saunders (Canadian) side of the dam in 1974 and a second eel

ladder was installed in 2006 on the Moses (US) side of the dam. Data were available from 1979 to 1995 and 2006 to 2018 (omitting 2016 and 2017). The more recent data included counts from both the Saunders and Moses ladders, which were combined. Because of the large time gap and the addition of the Moses ladder two models were produced. Potential covariates for both models were the same and included month, temperature as up to a second degree polynomial, precipitation, water level as up to a second degree polynomial, and lunar phase.

Sub-annual temporal trends were included as potential random effects for both models, using an rw2 structure, to account for variation in catch within a year. The various random effect structures explored were: no additional random effects ($z_j = 0$), month as a random effect ($z_j = month_j$), week as a random effect ($z_j = week_j$) and day of the year as a random effect ($z_j = day_j$); in addition, fits were made with the month or week random effect being allowed to varying among years ($z_{jt} = month_{jt}$ or $z_{jt} = week_{jt}$), which allows the intra-annual trend to be different each year. A year-varying day random effect was not fit as the number of random effects would exceed the number of data points. When sub-annual temporal trends were included in the model fit month was not included as a fixed effect.

Beauharnois Eel Ladder

The Beauharnois Dam is located on the St. Lawrence River near Montreal. Eel ladders were installed in 2002 (west side) and 2004 (east side) to allow upstream passage. Daily counts of eels passing over the ladders were used as the response variables. Counts were summed across the two (east and west) ladders and a single model was produced. Observations from June were excluded as they were mostly zeros. Potential covariates included month (July to October), temperature as up to a second degree polynomial, precipitation, flow, and lunar phase.

Sub-annual temporal trends were included as potential random effects, using an rw2 structure, to account for variation in catch within a year. The various random effect structures explored were: no additional random effects ($z_j = 0$), month as a random effect ($z_j = month_j$), week as a random effect ($z_j = week_j$) and day of the year as a random effect ($z_j = day_j$); in addition, fits were made with the random month or week random effect being allowed to varying among years ($z_{jt} = month_{jt}$ or $z_{jt} = week_{jt}$), which allows the intra-annual trend to be different each year. A year-varying day random effect was not fit as the number of random effects would exceed the number of data points. When sub-annual temporal trends were included in the model fit month was not included as a fixed effect.

Chambly Eel Ladder

The Chambly Dam is located on the Richelieu River (river km 70). An eel ladder was installed in the late 1990s to allow upstream passage. Data were available from 2004 to 2018. Daily counts of eels passing through the ladder was used as a response variable. Potential covariates included temperature as, up to, a second degree polynomial, flow ($\log_e$-transformed to reduce the impact of large values), month, and lunar phase.

Sub-annual temporal trends were included as potential random effects, using an rw2 structure, to account for variation in catch within a year. The various random effect structures explored were: no additional random effects ($z_j = 0$), month as a random effect ($z_j = month_j$), week as a random effect ($z_j = week_j$) and day of the year as a random effect ($z_j = day_j$); in addition, fits were made with the random month or week random effect being allowed to varying among years ($z_{jt} = month_{jt}$ or $z_{jt} = week_{jt}$), which allows the intra-annual trend to be different each year. A year-varying day random effect was not fit as the number of random effects would

exceed the number of data points. When sub-annual temporal trends were included in the model fit month was not included as a fixed effect.

St. Nicholas Trap

The Nicholas Trap dataset comes from a monitoring program in the St. Lawrence Estuary near Quebec City. An estuary trap, similar to commercial gear, was used, however, with a finer mesh. Data were available from 1975 to 2018, however, 2015 and 2016 were missing. Data were limited to months September and October as catch in these months is likely to represent silver eels (Cornic et al. 2021). In recent years, a significant proportion of the silver eel captured in the survey had been translocated as glass eel from the east coast between 2005 and 2010 in a stocking effort (Landry-Massicotte et al. 2024). To ensure the trend represented in this analysis related solely to naturally occurring eel the catch in 2017 and 2018 were reduced by the estimated proportion of translocated silver eel in the run, 33.5 and 30.3%, respectively (Landry-Massicotte et al. 2024). Data were also limited to soak times between 11 and 14 hours for consistency. Eel count per trap was used as the response variable. Potential covariates included temperature as up to a second degree polynomial, river discharge, month, and lunar phase. Sampling effort varied among samples there $\log_e$(soak time) was used as an offset.

Sub-annual temporal trends were included as potential random effects, using an rw2 structure, to account for variation in catch within a year. The various random effect structures explored were: no additional random effects ($z_j = 0$), month as a random effect ($z_j = month_j$), week as a random effect ($z_j = week_j$) and day of the year as a random effect ($z_j = day_j$); in addition, fits were made with the random month or week random effect being allowed to varying among years ($z_{jt} = month_{jt}$ or $z_{jt} = week_{jt}$), which allows the intra-annual trend to be different each year. A year-varying day random effect was not fit as the number of random effects would exceed the number of data points. When sub-annual temporal trends were included in the model fit month was not included as a fixed effect.

Canada-wide trend

Annual estimates of relative abundance were extracted from the standardization models. Despite standardization, the time series remained on vastly different scales (e.g., catch-per-unit-effort from electrofishing time series or daily eel counts from eel ladder time series). To allow for an estimate of a Canada-wide trend in American Eel relative abundance the datasets must be transformed such that they are on similar scales. Three methods were used transform the response values. The first method was to $\log_e$-transform the data, where:

$$y = log_e(catch). \quad (6)$$

The second method was to scale the data by dividing each dataset by its standard deviation:

$$y = catch/\sigma_{catch}, \quad (7)$$

which results in each transformed dataset having a standard deviation of 1. And the third method was to normalize (feature scaling) the data, where:

$$y = \frac{catch - \min(catch)}{\max(catch) - \min(catch)}, \quad (8)$$

which results in each dataset having a range between 0 and 1.

Separate models were produced for each of the scaling methods. The models, however, were structured the same and included an intercept, α, and a $year$ trend (with $year$ centred). Random effects were included to account for potential dependencies at the location (dataset) and zone level and, in addition, a random slope effect was included by location to account for variation in

the slope among datasets. The $\log_e$-transformed response data were fairly normally distributed, continuous, and contained positive and negative values and were therefore modelled as a linear regression:

$$
\begin{aligned}
&y_{ilz} \sim Norm(\mu_{ilz}, \sigma) \\
&E(y_{ilz}) = \mu_{ilz} \\
&var(y_{ilz}) = \sigma \\
&\mu_{ilz} = \alpha + \beta_1 \cdot year + location_l + \gamma_l \cdot year + zone_z.
\end{aligned}
\tag{9}
$$

While the scaled and normalized response data were skewed, continuous and positive and were therefore modelled with a gamma probability distribution, where:

$$
\begin{aligned}
&y_{ilz} \sim Gamma(\mu_{ilz}, \kappa) \\
&E(y_{ilz}) = \mu_{ilz} \\
&var(y_{ilz}) = {\mu_{ilz}}^2/\kappa \\
&\log_e(\mu_{ilz}) = \alpha + \beta_1 \cdot year + location_l + \gamma_l \cdot year + zone_z.
\end{aligned}
\tag{10}
$$

Where κ is the shape parameter of the gamma distribution. Because of the logarithmic link or transformation the $year$ trend slope again represents r in the exponential model of population growth.

To investigate how the year trend has varied through time the above transformation and model fits were made for three temporal subsets of the data. The first fit included all datasets in their entirety, the second fit excluded data prior to 1980, and the third fit excluded data prior to 2000.

To investigate how much the standardization models influenced the results of this analysis the same model fits were made for the raw (unstandardized) data. Annual arithmetic means were taken from each dataset accounting for only variation in sampling effort.

These analyses were conducted using all twelve datasets to represent a Canada-wide trend for American Eel in freshwater using all available data. As well, the analyses were conducted using only the ten datasets targeting the yellow eel stage to provide a trend without life-stage as a potential confounding factor.

The various American Eel zones represent vastly different amounts of available habitat (Cairns et al. 2014, Figure 2) and could therefore represent different proportions of the total American Eel population in Canada. To account for this the relative proportion of total habitat was calculated for each zone (Scotia Fundy = 0.1065, Southern Gulf = 0.0465, Northern Gulf = 0.397, and St. Lawrence Basin = 0.450, Cairns et al. 2014) and this value was used as a weight for each dataset within each zone in the model fit. This was repeated with the proportion of total habitat divided by the number of datasets within the zone to attempt to account for the uneven number of datasets representing the different zones (this is potentially accounted for already with inclusion of the $zone$ random effect). While including weights is an option with INLA the help files include a warning stating that the normalizing constant is not recomputed and all marginals must be interpreted with care. Therefore it is not clear if estimates from these model fits are reliable.

Finally, to further investigate the influence of uneven zone representation among datasets the models were refit with a single dataset sampled from each zone, termed sample analysis. Here only four datasets were included in a model fit and all possible combinations of datasets were analysed. As well, to investigate the influence each dataset had on the model outputs the model was refit while excluding each dataset individually, termed leave-one-out analysis.

Dynamic Factor Analysis

An additional analysis, dynamic factor analysis (DFA), was performed to inform the Canada-wide American Eel population trend. DFA is a dimension reduction procedure for time series that reduces n time series to m common trends (Holmes et al 2024b):

$$\boldsymbol{y}_t = \boldsymbol{Z}\boldsymbol{x}_t + \boldsymbol{v}_t \; where \; \boldsymbol{v}_t \sim MVN(0, \boldsymbol{R}) \quad (11)$$

$$\boldsymbol{x}_t = \boldsymbol{x}_{t-1} + \boldsymbol{w}_t \; where \; \boldsymbol{w}_t \sim MVN(0, \boldsymbol{I}).$$

Where $\boldsymbol{y}$ is a matrix of the time series, $\boldsymbol{x}$ are the latent trends, here a random walk, $\boldsymbol{Z}$ is an $n \times m$ matrix of factor loadings, and $\boldsymbol{v}$ and $\boldsymbol{w}$ are error terms, $\boldsymbol{w}$ is fixed as an identity matrix while $\boldsymbol{R}$ can take various forms.

DFA models were fit to the standardized and raw annualized datasets for years 1980-2018. The data were centred and scaled, which is required for application of DFA models. Models with 1 to 4 latent trends were considered and three covariance structures, $\boldsymbol{R}$, were explored. The covariance structures were: independent with equal variance, independent with unequal variance, and compound symmetric by zone, where there is a dependency among time series within each zone. The preferred number of latent trends and covariance structure was selected as the model with the lowest AICc that correctly converged after 20,000 iterations.

RESULTS

STANDARDIZATION MODELS

Scotia Fundy

LaHave River Electrofishing

Table 3. LaHave River electrofishing dataset standardization model parameter estimates. The selected model included a zero-inflated negative binomial probability distribution and tributary as a random intercept. See Table 2 and Equations 1-3 for parameter definitions.

Parameters	Mean	SD	LCI	UCI
Fixed Effects				
Intercept	-5.709	0.38	-6.508	-4.986
Year	-0.033	0.043	-0.121	0.056
Temperature	-0.181	0.094	-0.364	0.004
Hyperparameters				
k	1.069	0.181	0.751	1.459
π	0.163	0.038	0.095	0.241
$\sigma_{tributary}$	0.788	0.264	0.386	1.411
σ_{year}	0.725	0.212	0.403	1.229
ρ	0.611	0.206	0.127	0.909

The selected model structure used a zero-inflated negative binomial probability distribution with tributary as a random intercept. This model structure may produce slight under-dispersion based on SSE and residual variance Bayesian p-values but was an improvement over models that included site as a random effect (Table A1.1). A model omitting additional random effects following a negative binomial probability distribution may represent an alternative but produced a larger WAIC ($\Delta WAIC = 24$). The selected model produced an appropriate number of 0s (Table A1.1) and there was no pattern visible in the residuals (Figure A1.1).

Temperature was the only covariate maintained in the final model; the coefficient slope was negative, however, the 95% coefficient credible intervals (CI) did overlap 0 (Table 3). The year slope was negative but not important (95% CIs overlapped 0), indicating there has not been a significant decline in eel count over the course of the survey.

A standardized annual index of abundance was output from the model as the mean eel count per 100 m^2 electrofishing pass, at the mean temperature, and independent of tributary.

Nashwaak River Electrofishing

The selected model structure used a zero-inflated negative binomial probability distribution with site as a random intercept (Table A1.2). This model structure produced reasonable fit statistics except for the SSE Bayesian p-value which may indicate some under-dispersion. There were, however, an appropriate number of zeros produced by the model and no visible pattern in the model residuals (Figure A1.1). The model with a ZINB and no additional random effects may represent an alternative structure but produced a larger WAIC ($\Delta WAIC = 25$).

Temperature was the only covariate maintained in the final model; the coefficient slope was positive (opposite to the LaHave River model), and the 95% coefficient credible intervals (CI) differed from 0 (Table 4). The year slope was negative and different from 0 indicated a significant decline in eel count over the course of the survey. The estimated decline was ~3% (95% CI: 5.3 - 0.5%) per year indicating a > 60% (95% CI: 80.1-14.3%) decline over the 31 year time series.

A standardized annual index of abundance was output from the model as the mean eel count per 100 m^2 electrofishing pass, at the mean temperature, and independent of site.

Table 4. Nashwaak River electrofishing dataset standardization model parameter estimates. The selected model included a zero-inflated negative binomial probability distribution and site as a random intercept. See Table 2 and Equations 1-3 for parameter definitions.

Parameters	Mean	SD	LCI	UCI
Fixed Effects				
Intercept	-4.254	0.106	-4.463	-4.041
Year	-0.03	0.012	-0.056	-0.005
Temperature	0.13	0.04	0.053	0.208
Hyperparameters				
k	3.704	0.402	2.975	4.547
π	0.1	0.016	0.07	0.134
σ_{site}	0.39	0.098	0.236	0.617
σ_{year}	0.386	0.076	0.261	0.56
ρ	0.359	0.23	-0.111	0.764

St. Mary's River

The selected model structure used a zero-inflated negative binomial probability distribution with site as a random intercept (Table A1.3). This model structure produced reasonable fit statistics except for the SSE Bayesian p-value which may indicate some under-dispersion. There were, however, an appropriate number of zeros produced by the model and no visible pattern in the model residuals (Figure A1.1). The model with a ZINB and no additional random effects may represent an alternative structure but produced a larger WAIC ($\Delta WAIC = 102.6$).

Table 5. St. Marys River electrofishing dataset standardization model parameter estimates. The selected model included a zero-inflated negative binomial probability distribution and site as a random intercept. See Table 2 and Equations 1-3 for parameter definitions.

Parameters	Mean	SD	LCI	UCI
Fixed Effects				
Intercept	-3.964	0.123	-4.206	-3.719
Year	-0.08	0.039	-0.158	0.002
$\log_e$(Flow)	-0.148	0.063	-0.271	-0.023
Hyperparameters				
k	3.34	0.37	2.677	4.124
π	0.023	0.009	0.009	0.045
σ_{site}	0.537	0.102	0.37	0.768
σ_{year}	0.701	0.189	0.437	1.169
ρ	0.709	0.139	0.397	0.923

Flow ($\log_e$-transformed) was the only covariate maintained in the final model; the coefficient slope was negative and differed from 0 (Table 5). The year slope was negative and steeper than the LaHave or Nashwaak rivers estimate but a larger standard deviation indicated some uncertainty and the 95% CIs just overlapped 0. The posterior marginals indicated that the probability a decline has occurred (year slope < 0) is 97.3% and that the mean estimate of the proportional decrease in abundance was 84% (95% CIs: 97.4% decrease – 4.7% increase) over the 23 year time series.

A standardized annual index of abundance was output from the model as the mean eel count per 100 m^2 electrofishing pass, at the mean $\log_e$(flow), and independent of site.

East River Elver Trap

Table 6. East River, Chester, NS elver trap dataset standardization model parameter estimates. The selected model included a zero-inflated negative binomial probability distribution and month as a random intercept with the month effect allowed to vary among years. See Table 2 and Equations 1-3 for parameter definitions.

Parameters	Mean	SD	LCI	UCI
Fixed Effects				
Intercept	8.799	0.236	8.345	9.272
Year	0.067	0.062	-0.055	0.195
Tide	-0.313	0.068	-0.447	-0.18
Lunar Phase	0.211	0.049	0.116	0.306
Hyperparameters				
k	0.513	0.02	0.475	0.554
π	0.032	0.005	0.024	0.044
σ_{month}	2.951	0.263	2.357	3.318
σ_{year}	1.012	0.375	0.495	1.948
ρ	0.773	0.17	0.33	0.969

The selected model structure used a zero-inflated negative binomial probability distribution with a random intercept for month where the month effect was allowed to vary among years (Table A1.4). The SSE and residual variance indicate potential under-dispersion, however, the number of zeros produced by the model was appropriate and there was no visible pattern in the residuals (Figure A1.1). None of the other explored model structures produced reasonable alternatives based on the fit statistics.

Tide height and lunar phase were maintained as important covariates in the final model (Table 6). Elver count decreased with tide height and increased with lunar phase. The year slope was positive but the 95% CIs bounded 0. The posterior marginals of the year slope indicated that there was a 87.5% likelihood that there has been an increase in the daily elver count over the time series.

A standardized annual index of abundance was output from the model as the mean eel count per day taken as the average over May and June to account for shifting peaks among years, at the mean tide height and lunar phase.

Southern Gulf

Miramichi River

The selected model structure used a negative binomial probability distribution with site as a random intercept (Table A2.1). This model structure may be under-dispersed and produced too few 0s relative to the observed data. There was a slight trend in the residuals, increasing at larger fitted values, indicating the model may produce underestimates for larger observed values. Using a ZINB distribution provided no improvement in dispersion or 0s. Excluding site as a random effect improved the fit statistics but gave a much higher WIAC ($\Delta WAIC = 465.4$). It was determined that repeat site visits likely represent an important grouping factor in the data, which was supported by the large standard deviation estimate associated with this random effect (Table 7), and therefore it was maintained in the model.

Table 7. Miramichi River electrofishing dataset standardization model parameter estimates. The selected model included a negative binomial probability distribution and site as a random intercept. See Table 2 and Equations 1-3 for parameter definitions.

Parameters	Mean	SD	LCI	UCI
Fixed Effects				
Intercept	-6.021	0.141	-6.305	-5.751
Year	-0.017	0.006	-0.029	-0.005
$\log_e$(Flow)	-0.334	0.08	-0.492	-0.176
Longitude	0.301	0.114	0.075	0.522
Hyperparameters				
k	0.268	0.014	0.241	0.296
σ_{site}	1.398	0.116	1.188	1.645
σ_{year}	0.524	0.082	0.379	0.701
ρ	0.255	0.203	-0.164	0.621

Flow ($\log_e$-transformed) and longitude were maintained in the model as important covariates (Table 7). Eel count decreased with flow and increase at locations closer to the mouth of the river. The year trend was negative and different from 0. The mean estimate of the proportional decrease in abundance over the 67 year time series was 68% (95%CIs: 85.6% – 28.5%). When site was not included as a random effect, however, the year slope did not differ from 0 (-0.004, 95%CI: -0.17 – 0.01).

A standardized annual index of abundance was output from the model as the mean eel count per 100 m^2 electrofishing pass, at the mean $\log_e$(flow) and longitude, and independent of site.

Restigouche River

The selected model structure used a Tweedie probability distribution with site as a random intercept (Table A2.2). This model structure produced too few zeros (mean 1,810 compared to 1,919 in the observed data) but the other fit statistics were satisfactory and there was no

significant pattern in the residuals (Figure A2.1). An alternative model structure could use the ZINB distribution and maintain site as a random effect. This distribution produced a lower WAIC ($\Delta WAIC = -89.1$) and the appropriate number of zeros but worse dispersion related fit statistics and a trend was present in the residuals plots. Excluding site as a random effect, with a ZINB probability distribution, improved the fit statistics but gave a much higher WIAC ($\Delta WAIC = 410$) and there was a notable pattern in the residual plot.

Temperature was maintained as an important covariate (Table 8). The year slope was negative and different from 0. The mean estimate of the proportional decrease in abundance over the 47 year time series was 85.4% (95%CIs: 94.7% – 62.6%). The year slope was similar when a ZINB probability distribution was used (-0.044, 95% CI: -0.068 – 0.02). When site was omitted as a random effect, however, the year slope was significantly positive (0.065, 95% CIs: 0.040 – 0.086). This result is likely driven by the increase in variance in catch observed in the latter part of the time series (after 1994, Figure 3), leading to issues with model fit (e.g., pattern in the residual plot).

A standardized annual index of abundance was output from the model as the mean eel count per 100 m^2 electrofishing pass and independent of site.

Table 8. Restigouche River electrofishing dataset standardization model parameter estimates. The selected model included a zero-inflated negative binomial probability distribution and site as a random intercept. See Table 2 and Equations 1-3 for parameter definitions.

Parameters	Mean	SD	LCI	UCI
Fixed Effects				
Intercept	-8.310	0.449	-9.269	-7.501
Year	-0.041	0.010	-0.062	-0.021
Temperature	0.142	0.059	0.026	0.258
Hyperparameters				
k	1.344	0.013	1.319	1.37
π	3.697	0.121	3.466	3.94
σ_{site}	3.123	0.32	2.542	3.796
σ_{year}	0.507	0.093	0.347	0.709
ρ	0.387	0.191	-0.018	0.717

Northern Gulf

Sud Ouest River Trap

The selected model structure used a negative binomial probability distribution with a random intercept for month where the month effect was allowed to vary among years (Table A3.1). This model structure produced adequate fit statistics and there was no visible pattern in the residual plots (Figure A3.1)

Precipitation, temperature as a second degree polynomial, and lunar phase were maintained in the final model (Table 9). Eel count increased slightly with precipitation and greatly at increased temperatures but decreased with lunar phase. The year trend was positive but did not differ from 0.

A standardized annual index of abundance was output from the model as the mean eel count per day taken as the average across months to account for shifting peaks among years, at the mean precipitation and temperature.

Table 9. Sud Ouest River trap dataset standardization model parameter estimates. The selected model included a negative binomial probability distribution and month as a random intercept with the month effect allowed to vary among years. See Table 2 and Equations 1-3 for parameter definitions.

Parameters	Mean	SD	LCI	UCI
Fixed Effects				
Intercept	1.41	0.123	1.176	1.657
Year	0.068	0.049	-0.036	0.165
Precipitation	0.11	0.052	0.008	0.213
Temperature	0.92	0.081	0.762	1.08
Temperature^2	0.248	0.039	0.17	0.325
Lunar Phase	-0.145	0.051	-0.246	-0.044
Hyperparameters				
k	0.532	0.028	0.477	0.588
σ_{month}	2.261	0.383	1.626	3.126
σ_{year}	0.818	0.183	0.521	1.238
ρ	-0.065	0.434	-0.8	0.755

St. Lawrence Basin

Bay of Quinte

The selected model structure used a negative binomial probability distribution with no additional random effects (Table A4.1). This structure produced slightly high dispersion fit statistics, potentially because of the consecutive 0 observations in later years of the time series, but produced an appropriate amount of 0s and there was no visible pattern in the residuals (Figure A4.1). Including site as a random effect did not improve model fit ($\Delta WAIC > -2$).

Table 10. Bay of Quinte trawl dataset standardization model parameter estimates. The selected model included a zero-inflated negative binomial probability distribution and site as a random intercept. See Table 2 and Equations 1-3 for parameter definitions.

Parameters	Mean	SD	LCI	UCI
Fixed Effects				
Intercept	-0.938	0.215	-1.367	-0.523
Year	-0.152	0.029	-0.208	-0.088
June	-0.501	0.209	-0.911	-0.091
July	-0.645	0.237	-1.11	-0.179
August	-0.646	0.199	-1.036	-0.254
September	-0.724	0.229	-1.173	-0.275
October	-2.007	0.288	-2.572	-1.441
Depth	0.109	0.05	0.011	0.206
Hyperparameters				
k	0.877	0.093	0.71	1.073
σ_{year}	1.127	0.257	0.722	1.725
ρ	0.678	0.143	0.343	0.892

Month and depth were maintained in the final model (Table 10). Catch was greatest in May and lowest in October and increased slightly over the range of depths sampled (3.0 to 9.14 m). The year trend was steep and significant. The estimated decline was 14.1% (95%CI: 18.8 – 8.4%) per year indicating a > 99.9% decrease in catch over the 46 year time series.

A standardized annual index of abundance was output from the model as the mean eel count per trawl at the mean depth in August.

Moses-Saunders Eel Ladder

The Saunders eel ladder time series was split into two datasets with individual models created because of a time gap and addition of the Moses ladder. The 1979-1995 model used a model structure that included a zero-inflated negative binomial probability distribution with week as a random intercept with the week effect constant across years (Table A4.2). The 2006-2018 model used a model structure with a negative binomial probability distribution with day as a random intercept held constant across years (Table A4.3). There were issues with model fit for both models, however, alternative model structures did not result in any improvements. There was also a visible pattern in the residuals, which may indicate over-fitting to larger observed values (a convergence of residuals to 50% at greater predicted values; Figure A4.1). As such, model results may be tentative.

Table 11. Saunders eel ladder datasets standardization models parameter estimates (1979-1995 and 2006-2018). The selected models included a zero-inflated negative binomial and a negative binomial probability distribution, respectively, with week as a random intercept held constant across years. See Table 2 and Equations 1-3 for parameter definitions.

Parameters	Mean	SD	LCI	UCI
1979 to 1995				
Fixed Effects				
Intercept	6.518	0.074	6.375	6.662
Year	-0.201	0.074	-0.344	-0.042
Water Level	0.153	0.052	0.052	0.255
Water Level^2	0.163	0.032	0.099	0.226
Hyperparameters				
k	1.388	0.054	1.286	1.492
π	0.219	0.011	0.199	0.241
σ_{week}	0.500	0.156	0.243	0.886
σ_{year}	1.137	0.245	0.751	1.709
ρ	0.277	0.255	-0.261	0.709
2006 to 2018				
Fixed Effects				
Intercept	4.765	0.062	4.644	4.89
Year	-0.011	0.095	-0.193	0.195
Temperature	0.185	0.045	0.097	0.273
Temperature^2	0.068	0.026	0.016	0.12
Hyperparameters				
k	0.851	0.031	0.792	0.912
σ_{day}	0.029	0.008	0.016	0.049
σ_{year}	0.875	0.267	0.509	1.542
ρ	0.608	0.209	0.135	0.918

Covariates differed between the models with water level as a second degree polynomial and temperature as a second degree polynomial maintained in the respective models (Table 11). The year trend also differed between the two time periods. There was a sharp and significant decline in eel count in the earlier time series while no change in eel count was found in the later time series. Between 1979 and 1995 the estimated decline was 20.1% (95%CI: 34.4 – 4.2%)

per year indicating a 96.7% (95%C: 99.7 – 51.0%) decrease in catch over the 17 year time series. A decline in eel count likely continued between 1995 and 2006 (Figure 3).

A standardized annual index of abundance was output from the models as the mean eel count per day at the mean temperature and water level in the 27th week of the year. The standardized dataset was treated as one dataset.

Beauharnois Eel Ladder

The selected model structure used the Tweedie probability distribution with day (constant across years) as a random intercept. This model structure produced good dispersion fit statistics but allowed for too few zero estimates (Table A4.4). There were 51 zeros in the dataset while the model could produce between 5 and 39 zeros (median = 18). Alternative model structures using a zero-inflated negative binomial distribution gave a more appropriate number of zeros and a lower WAIC, however, were substantially under-dispersed. There was a slight pattern and a number of outliers in the residual plot at larger fitted values indicating the model may be underestimating larger observed values.

Temperature as a second degree polynomial was maintained in the final model (Table 12), with eel count estimated to increase at a declining rate with temperature. The year trend was slightly negative but did not differ from 0. The posterior marginals of the year slope indicated there was a 68.2% likelihood that there has been a decrease in the daily eel count over the time series.

A standardized annual index of abundance was output from the models as the mean eel count per day at the mean temperature on the in 194th day of the year.

Table 12. Beauharnois eel ladder dataset standardization model parameter estimates. The selected model included a Tweedie probability distribution and day of the year as a random intercept. See Table 2 and Equations 1-3 for parameter definitions.

Parameters	Mean	SD	LCI	UCI
Fixed Effects				
Intercept	5.483	0.045	5.395	5.571
Year	-0.016	0.064	-0.129	0.143
Temperature	0.638	0.052	0.537	0.74
Temperature^2	-0.102	0.027	-0.156	-0.048
Hyperparameters				
p	1.701	0.008	1.686	1.718
ϕ	3.038	0.116	2.804	3.259
σ_{day}	0.017	0.004	0.009	0.026
σ_{year}	0.729	0.256	0.44	1.405
ρ	0.521	0.183	0.163	0.846

Chambly Eel Ladder

The selected model structure used the negative binomial probability distribution with month as a time varying (by year) random intercept. This model structure produced good dispersion fit statistics but allowed for too many zero estimates (Table A4.5). The dataset contained 337 observed 0s and across simulations the model generated 316 to 425 (median = 370) zeros. Alternative model structures did not provide improvements in any fit statistics. There were no visible patterns in the model residuals (Figure A4.1).

Table 13. Chambly eel ladder dataset standardization model parameter estimates. The selected model included a Tweedie probability distribution and day of the year as a random intercept. See Table 2 and Equations 1-3 for parameter definitions.

Parameters	Mean	SD	LCI	UCI
Fixed Effects				
Intercept	1.599	0.08	1.439	1.754
Year	0.014	0.071	-0.134	0.152
Temperature	1.152	0.055	1.043	1.26
Temperature ^{2}	0.136	0.034	0.07	0.202
$\log_e$(Flow)	0.262	0.121	0.025	0.499
Hyperparameters				
k	0.866	0.039	0.793	0.944
σ_{month}	0.885	0.133	0.661	1.18
σ_{year}	1.08	0.211	0.728	1.556
ρ	-0.037	0.247	-0.486	0.459

Temperature as a second degree polynomial and $\log_e$-transformed flow were maintained in the final model (Table 13). Eel count increased at an increasing rate with temperature and also increased at greater flows. The year slope was positive but not different from 0. The posterior marginals of the year slope indicated there was a 59.4% likelihood that there has been an increase in the daily eel count over the time series.

A standardized annual index of abundance was output from the model as the mean eel count per day taken as the average across months to account for shifting peaks among years, at the mean temperature and $\log_e$(flow).

St. Nicholas Trap

The selected model structure used the negative binomial probability distribution with day as a random intercept. This model structure may be over-dispersed based on the estimated fit statistics (Table A4.6) but produced an appropriate amount of 0s and there was no apparent trend in the residuals (Figure A4.1). None of the alternative model structures provided improvements to the fit statistics. Over-dispersion can lead to narrow model parameter CIs, as such, they should be interpreted with caution.

Table 14. St. Nicolas trap dataset standardization model parameter estimates. The selected model included a negative binomial probability distribution and day of the year as a random intercept. See Table 2 and Equations 1-3 for parameter definitions.

Parameters	Mean	SD	LCI	UCI
Fixed Effects				
Intercept	-2.363	0.033	-2.428	-2.298
Year	-0.013	0.007	-0.028	0.00
Temperature	-0.135	0.033	-0.199	-0.071
Temperature ^{2}	-0.088	0.021	-0.13	-0.047
Lunar Phase	0.116	0.02	0.076	0.155
Hyperparameters				
k	0.957	0.039	0.883	1.036
σ_{day}	0.029	0.011	0.014	0.055
σ_{year}	0.259	0.049	0.179	0.371
ρ	0.668	0.134	0.366	0.88

Temperature as a second degree polynomial and lunar phase were maintained in the final model. Eel count followed a convex negative pattern with temperature. The year slope very nearly differed from 0, however, the presence of over-dispersion limits its interpretation.

A standardized annual index of abundance was output from the model as the mean eel count per 12 hour soak time, at mean temperature, on the 157th day of the year.

CANADA-WIDE TREND

Thirteen standardization models were fit to datasets from twelve freshwater locations in Canada. Across datasets, five (38%) had significantly negative year trends and zero had significantly positive trends. Generally, datasets with more historical data had more negative year trends (Figure 4). Five out of six (83%) datasets with data from before 1990 exhibited significant negative slopes. This included datasets across zones: Scotia Fundy, Southern Gulf, and St. Lawrence Basin. The greatest declines were observed in the St. Lawrence Basin zone. Of the datasets that commenced after 1990 (seven datasets), three had positive year trend estimates, although none differed from zero based on 95% credible intervals.

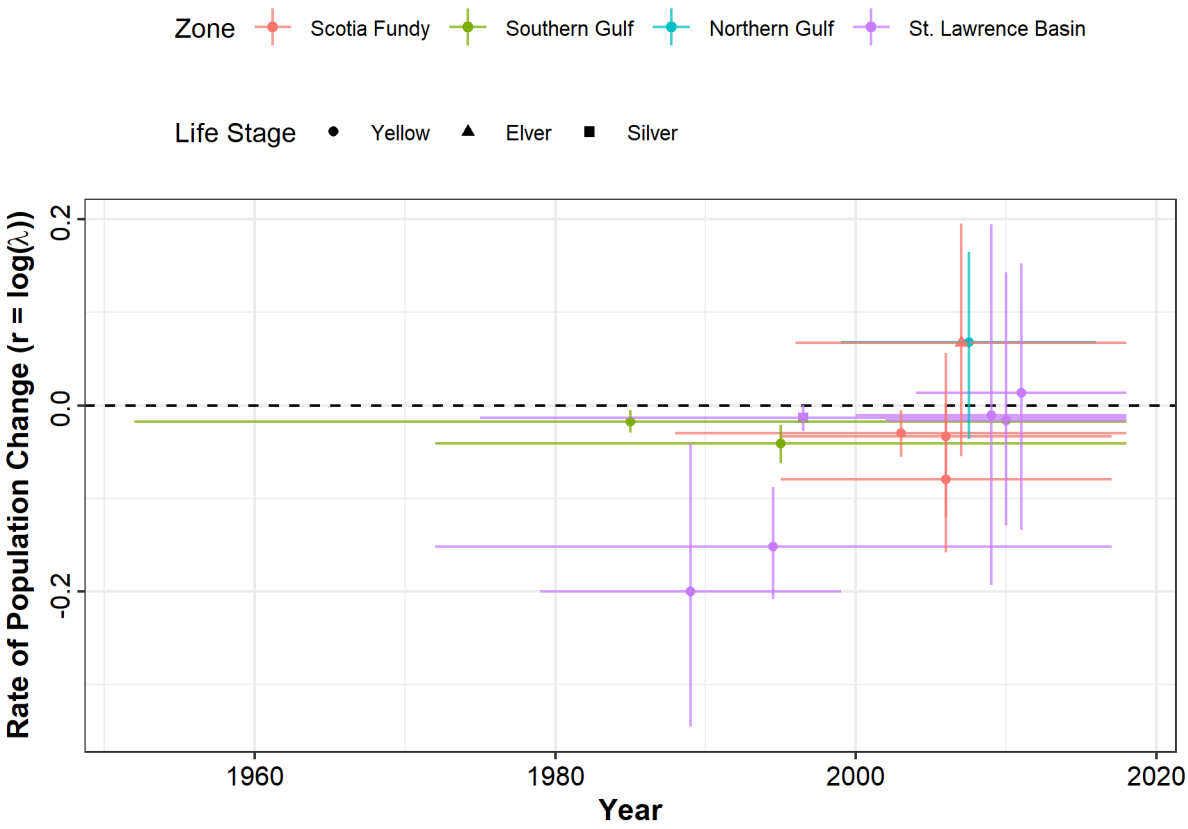

Figure 4. Estimates of the rate of population change from standardization models (Tables. 3-14) for each of the American Eel time series. Points represent the mid-point of the time series and mean estimate of r (year slope). Lines represent the range of sample years (x-axis) and 95% credible intervals of the r estimates (y-axis). Colour indicates the dataset zone.

Indices of annual relative abundance were generated from the standardization models. The indices generated from the standardization models were, for the most part, quite similar to indices from the raw data; however, often with reduced variability (Figure 5). The datasets from

the Southern Gulf zone are a notable exception, as they differed more significantly from the raw data.

Table 15. Canada-wide trend analysis results. Mean year slope (95% credible intervals) estimates for models fit to indices of relative abundance generated from standardization models and the raw data. Results are presented for three data transformation methods and fits to three temporal periods for all twelve time series and the ten time series targeting the yellow eel stage. Bold mean year slopes highlight the values that differ from zero.

	Time Series		
Model	**All**	**1980-2018**	**2000-2018**
All Datasets			
Standardized Data			
log-transformed	**-0.035 (-0.045, -0.024)**	**-0.035 (-0.046, -0.023)**	-0.012 (-0.028, 0.004)
Scaled	**-0.035 (-0.044, -0.025)**	**-0.032 (-0.043, -0.021)**	-0.012 (-0.028, 0.004)
Normalized	**-0.037 (-0.047, -0.027)**	**-0.035 (-0.047, -0.023)**	**-0.027 (-0.049, -0.006)**
Raw Data			
log-transformed	**-0.029 (-0.042, -0.015)**	**-0.027 (-0.041, -0.012)**	-0.010 (-0.03, 0.011)
Scaled	**-0.028 (-0.039, -0.018)**	**-0.025 (-0.039, -0.011)**	-0.011 (-0.036, 0.015)
Normalized	**-0.024 (-0.034, -0.015)**	**-0.021 (-0.034, -0.009)**	-0.014 (-0.035, 0.008)
Yellow Eel Datasets			
Standardized Data			
log-transformed	**-0.047 (-0.059, -0.034)**	**-0.046 (-0.06, -0.032)**	-0.015 (-0.033, 0.003)
Scaled	**-0.042 (-0.052, -0.033)**	**-0.042 (-0.055, -0.028)**	-0.016 (-0.033, 0.001)
Normalized	**-0.043 (-0.055, -0.033)**	**-0.045 (-0.06, -0.03)**	**-0.027 (-0.051, -0.003)**
Raw Data			
log-transformed	**-0.039 (-0.055, -0.023)**	**-0.037 (-0.054, -0.019)**	-0.010 (-0.033, 0.014)
Scaled	**-0.032 (-0.044, -0.021)**	**-0.033 (-0.049, -0.015)**	-0.009 (-0.038, 0.02)
Normalized	**-0.03 (-0.042, -0.018)**	**-0.03 (-0.045, -0.014)**	-0.012 (-0.036, 0.013)

The Canada-wide trend model fits produced similar results across the three methods used to transform/scale the datasets and between the models fit to standardized and raw abundance indices (Tables 15, A5.1 – A5.6, Figures 6, A5.1, A5.2). When fit to yellow eel specific time series the year trends were more negative than when all time series were included. All temporal trends, for models fit to the entire time series and from 1980-2018, produced significant negative slopes. Mean slopes ranged from -0.022 to -0.047. With all data sets included, there was a 69.2 to 99.6 % likelihood that American Eel abundance has declines > 50% since 1980 across standardized and raw data fits. When limited to yellow eel time series the probability increased to 92.8 to 100%. The likelihood that the decline since 1980 was > 70% was 6.0 to 66.8% with all data set included and 40.3 to 97.7 when the focus was yellow eel relative abundance (Figure 6). When the fit was limited to data from years 2000-2018 the year trend slopes were less negative and five of the six results did not differ from 0. For fits to the 2000-2018 data, estimates of decline were most probable, however, there exist the possibility of an increase in relative

abundance with a likelihood of 1 to 5% for fits to standardized data and 11 to 21% for fits to raw data for all time series and 1 to 4% and 17 to 27% for yellow eel time series.

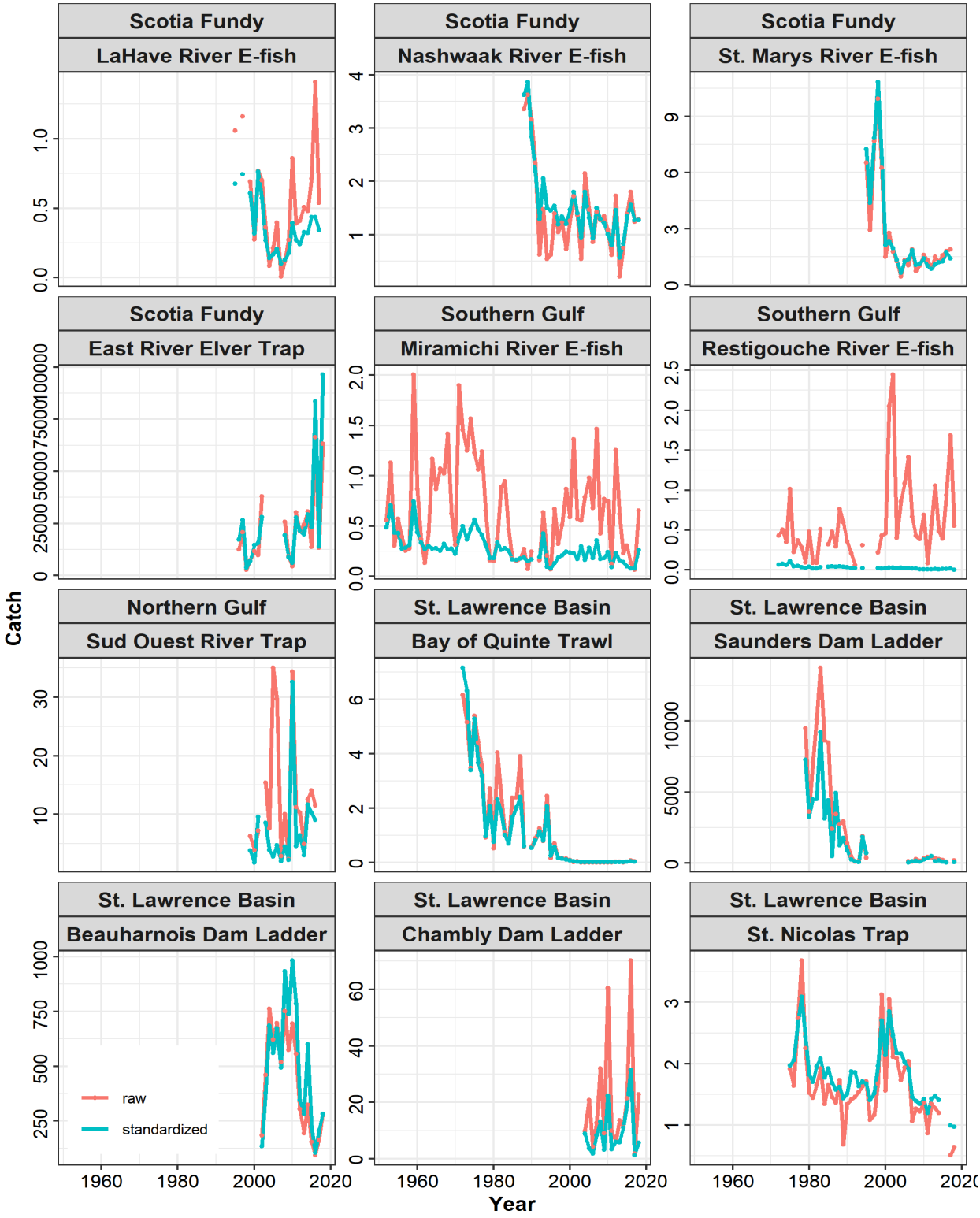

Figure 5. Annual relative abundance indices for each American Eel time series generated using the selected standardization model (blue) and from the raw data (red).

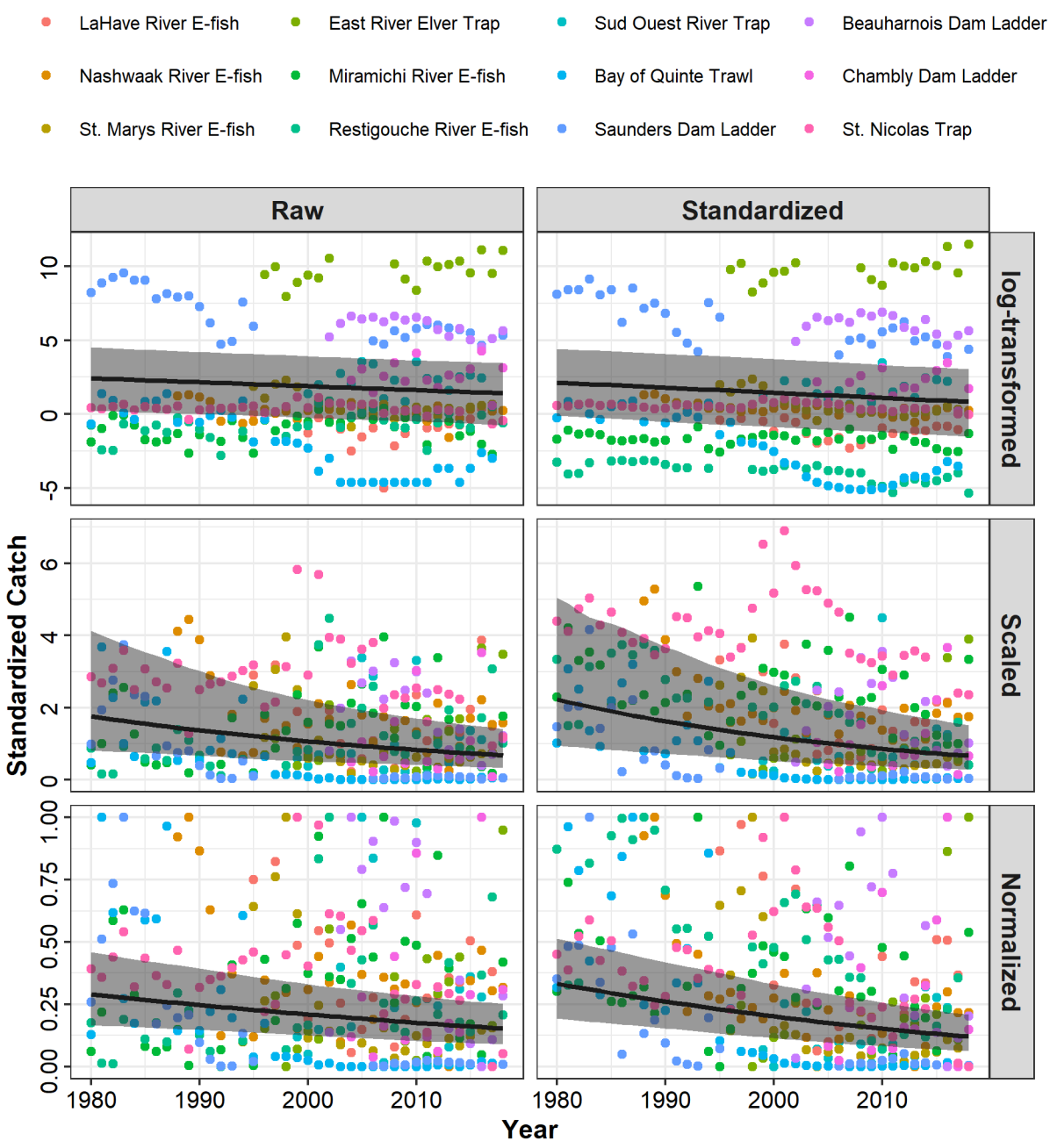

Figure 6. Canada-wide trend analysis results for models fit to raw and standardized indices of relative abundance from years 1980-2018. Three transformation methods were used to scale the datasets. The black line indicates the mean trend and the grey area indicates 95% credible intervals.

The standardized data from 1980-2018 including all datasets were refit to include weighting of zones by watershed size. This increases the emphasize on datasets from the St. Lawrence Basin and Northern Gulf zones. The result was a more negative slope, mean estimates ranged from -0.038 to -0.042 across transformation methods. When the weighting was scaled by the number of datasets from within each zone, the model was weighted most heavily towards the single Northern Gulf dataset, and the estimated mean slopes were slightly lower, -0.028 to -0.040.

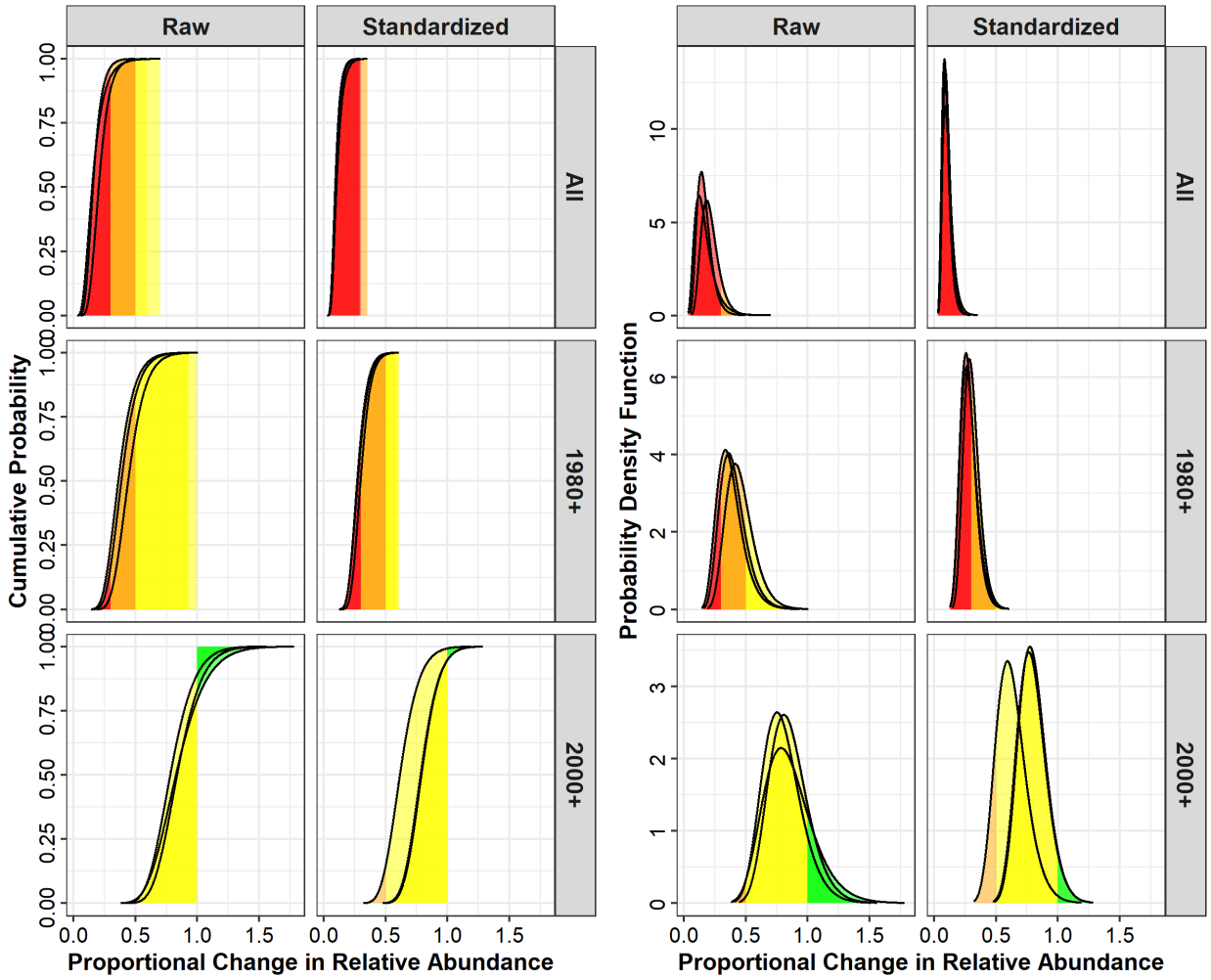

Figure 7. Cumulative probability (left) and probability density function (right) of levels of proportional population change for American Eel in Canada estimated for three temporal periods (All: 1952 to 2018; 1980+: 1980 to 2018; and 2000+: 2000 to 2018)I for standardized and raw data using all twelve America Eel data timeseries. The lines represents results for the three data transformation methods. Colours represents different levels of population change: red - > 70% decline, orange - 50-70% decline, yellow: decline < 50%, green: population increase.

The influence of the individual datasets and the uneven number of datasets among zones were investigated with sample and leave-one-out analysis. The sample analysis consisted of 40 model fits and included all unique combinations of datasets across zones (one from each). The Sud Ouest River trap dataset was included in all fits, as the only representative from the Northern Gulf zone, and demonstrates the full range of year slope estimates (Figure 8). Slopes ranged from -0.061 to 0.029. Eighteen slopes were significantly negative (45%) and two were significantly positive (5.0%). Both significant positive slopes included the East River elver trap dataset. When either the Saunders Eel Ladder or Bay of Quinte trawl datasets were included in the model fit the slope estimate was always negative, however, 3/16 were not significantly different from 0 (all non-significant estimates included the East River elver trap dataset as the Scotia-Fundy representative).

The leave-one-out analysis demonstrates the influence of individual datasets on the overall results. The leave-one-out analysis consisted of 12 addition model fits applied to the

standardized data, from years 1980-2018, transformed with scaling (Equation 7). The slope estimates ranged from -0.040 to -0.021 with a mean of -0.032. All estimates were significantly different from 0. The most negative slope occurred with the exclusion of the East River elver trap dataset. This dataset had the most positive year trend slope (Table 6) and was the only dataset representing the elver stage. The least negative slope occurred with the exclusion of the Bay of Quinte trawl dataset. The St. Nicolas trap dataset was the only dataset that represented silver eel and was the longest timeseries without a significant negative trend. When excluded from the model fit the slope was -0.034.

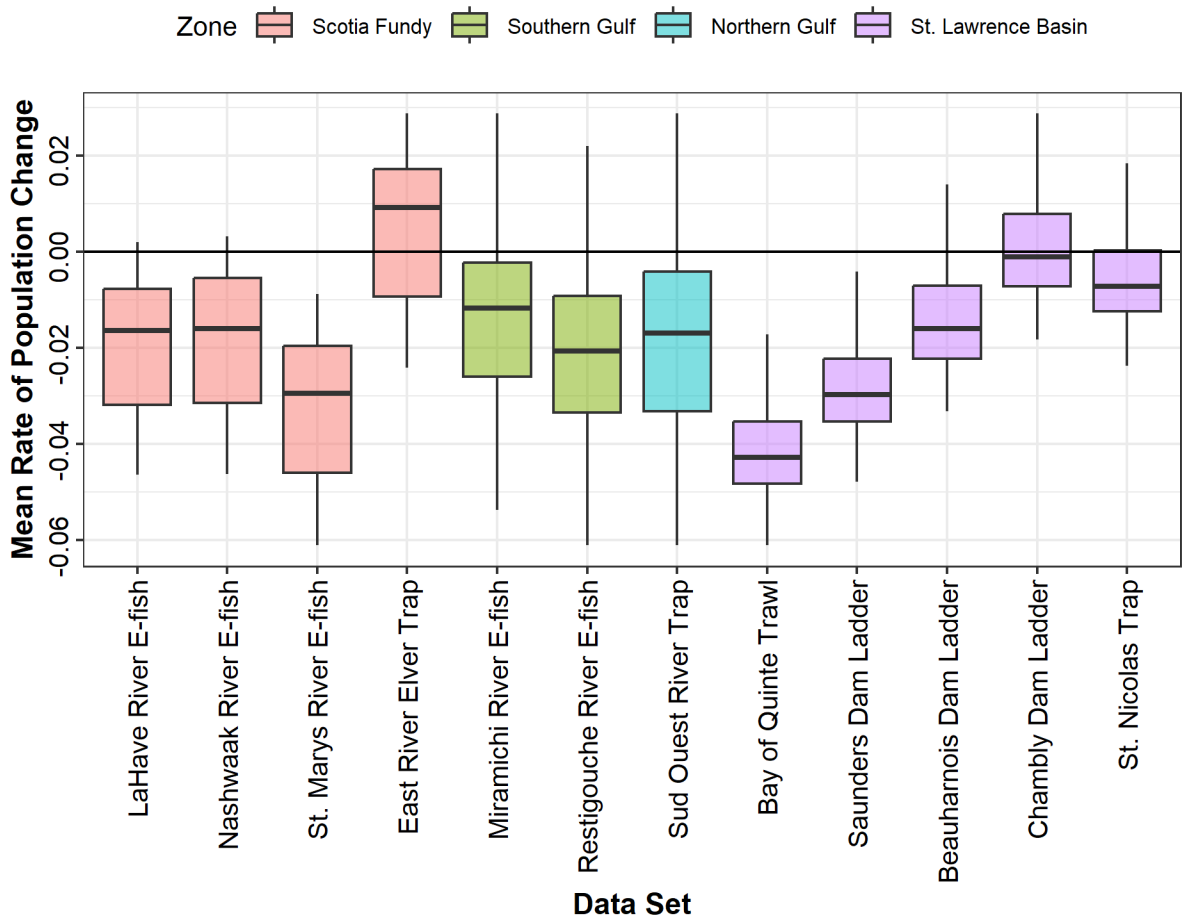

Figure 8. Results of sample analysis (one dataset sampled from each zone was included in analysis). The y-axis is the mean year slope from model results representing the instantaneous rate of population change ($\lambda = e^r$) when the dataset was included in the model fit. The analysis was applied to the standardized data, for years 1980-2018, transformed with scaling (Equation 7).

Dynamic Factor Analysis

The best fit DFA model, fit to 1980-2018 standardized data, included three latent trends with an independent and equal covariance structure (Figure 9). Fits with unequal variance and > 1 latent trends did not correctly converge after 20,000 iterations. The next best fit included three trends with a compound symmetry covariance structure however there was no support for the more complex structure (ΔAICc ~ 1). ΔAICc for a fit with four trends was 9.3.

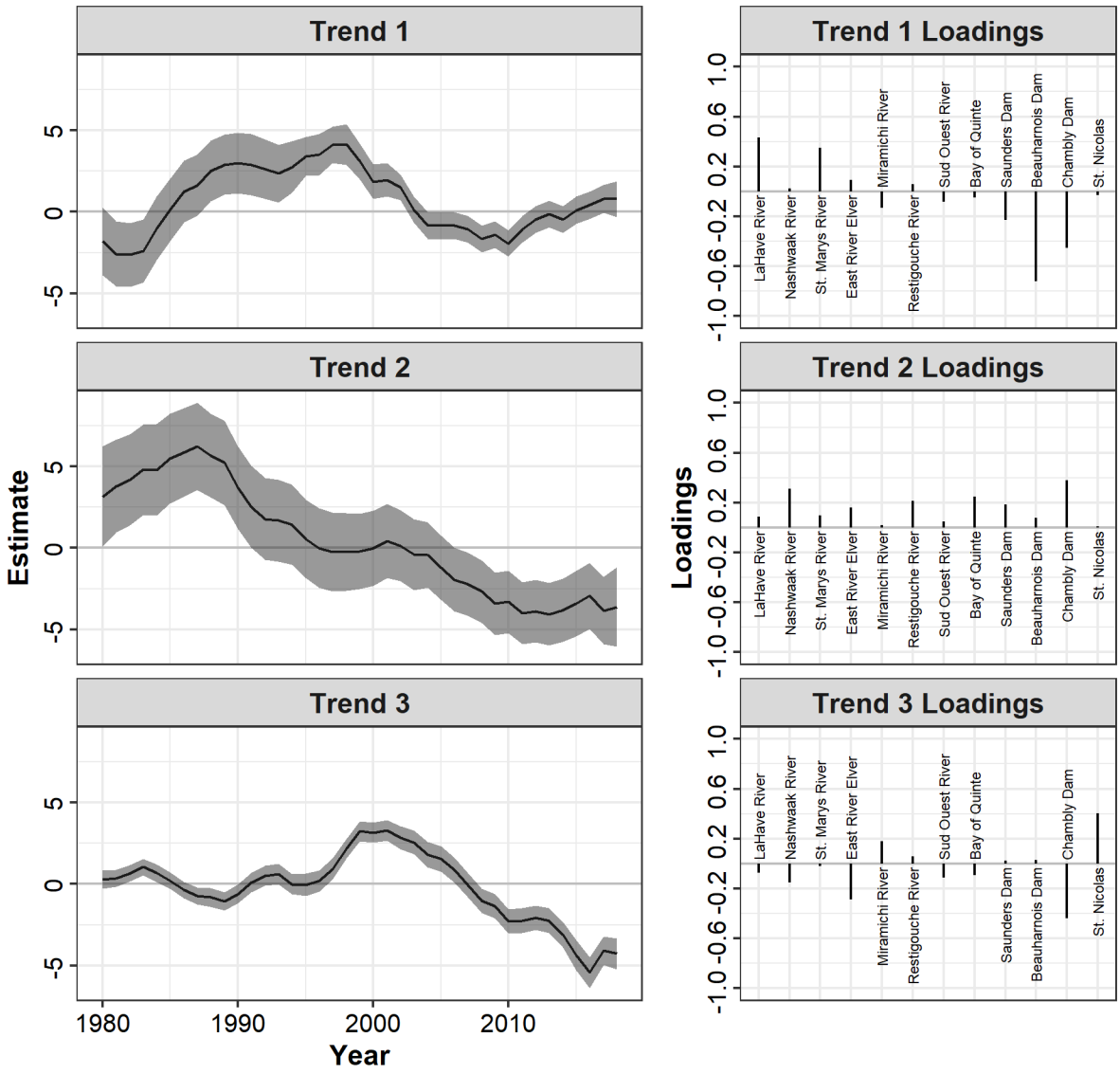

Figure 9. Dynamic factor analysis results fit to standardized data for years 1980-2018. The left column depicts the estimated trend lines and the right column depicts of the loading values associated with the trend line for each time series.

The loadings, $\boldsymbol{Z}$, of the trends (Figure 9) indicate the relative association of the time series to each trend line. A positive value indicates a positive association, the time series follows the trend, and a negative value indicates a negative association, the time series follows the inverse of the trend. Trend 1 indicates a potential periodicity to the time series, particularly LaHave River, St. Mary's River and Beauharnois Dam. None of these data sets have observations prior to 1995, as such, it is not clear what influenced the increase in the early years of this trend; perhaps it's the inverse of the Saunders dam trend. Trend 2 shows an almost continuous decline throughout the time series. The decline is steepest throughout the late 1980s and early 1990s and levels off in more recent years. All time series have positive loadings indicating that each could be associated with this declining trend. The interpretation of Trend 3 is less clear, it seems to closely follow the St. Nicolas trap trend line with some association with the increase observed from the East River elver trap time series. Chambly Dam had large loadings

associates with all three trends, which may indicate the Chambly Dam data are not well describes by the DFA model. When examining the time series specific predictions (Figure 10) it is evident that Chambly dam is poorly fit. There are additional fit issues, e.g. Bay of Quinte, and potential normality assumption violations which may impact the DFA model fit.

The DFA model fit to raw (unstandardized) data was similar to the standardized data fit with largely the same interpretation (Appendix 6).

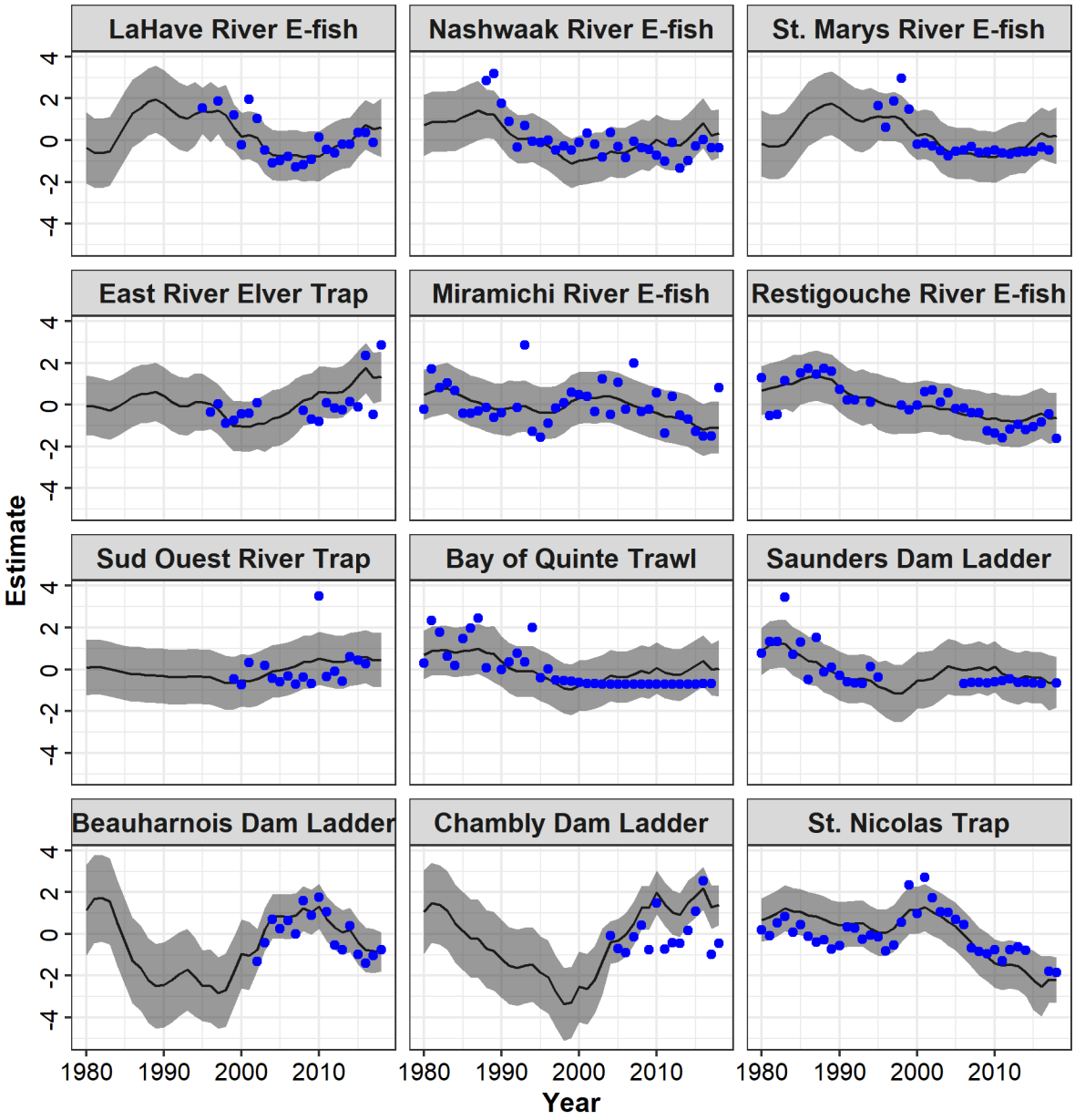

Figure 10. Time series-specific predictions from dynamic factor analysis fit to standardized data for years 1980-2018. The blue points are the data, the black lines are the mean predictions and the grey areas are the 95% confidence intervals.

DISCUSSION

The Canada-wide trend in relative abundance of American Eel was estimated by standardizing and amalgamating the various, long-term, fisheries-independent datasets, previously identified (Cairns 2020) to be informative of potential trends. The weight of evidence suggests that, throughout the freshwater Canadian range where data were available, the abundance of American Eel has declined. While the steepest and most dramatic declines occurred in the St. Lawrence Basin zone, smaller, but still significant declines were identified in the Scotia-Fundy and Southern Gulf zones as well. The main factor contributing to the finding of a significant decline in relative abundance was the start date of the time series. All datasets where a significant decline was estimated included sample years prior to 1990. No significant declines were identified in datasets commencing after 1990 and the Canada-wide trend estimates for years 2000-2018 were, predominantly, not different from 0. This indicates that, in freshwater in Canada, American Eel abundances have been relatively stable over the last two decades, but significant declines likely occurred previously and were not limited to the St. Lawrence Basin zone.

These results are broadly consistent with conclusions from previous trend analyses of American Eel abundances. Analyses that examined multiple time series regularly found mixes of declines and no change with some positive trends (Haro et al. 2000, COSEWIC 2012, Jacoby et al. 2017, ASMFC 2017, 2023, Cornic et al. 2021). The analyses presented here are the first to demonstrate the importance of including historical data to capture declines in American Eel abundances (Figure 4). Datasets included in this analysis have been used in previous analyses (Bowlby 2018, Cornic et al. 2021) and, for individual time series, the results are similar but not exactly the same due to differences in model structure.

Verreault and Dumont (2003) provided estimates of silver eel escapement from the upper St. Lawrence River and Lake Ontario for 1996 and 1997 with a 20% decline in escapement between these two years. This decline is consistent with the trend observed from the standardization model of the count data from the Moses-Saunders eel ladder (Table 11), even though the eel ladder counts represent eel ascending the river >10 years before they would again descend as silver eels.

This Canada-wide tend analysis is the first attempt to describe the overall trajectory of American Eel abundance in Canada. Comparison to the two available attempts for US data (ASMFC 2023, Kahn 2019) describe generally consistent patterns with declines through to the mid-1990s followed by a period of relatively stable abundances. ASMFC (2023) used a Gaussian state-space based approached to determine a common temporal trend across time series. The mean estimate for the rate of population change for yellow eel was negative but the confidence intervals overlapped 0. Time series-specific non-parametric Mann-Kendall trend test shows that negative trends were more common than positive among time series. The lack of evidence for a change in abundance post-2000 in the current analysis is consistent with the observations of shorter term time series reported by ASMFC (2017, 2023). Whereas, the index generated by Kahn (2019) shows possible recent increases in abundance. However, Kahn's index is based on recreational fishing data which represents inshore saltwater and brackish water, not freshwater. Furthermore, the low precision of the recreational fishery data and the limited numbers of American Eel encountered in these surveys (ASMFC 2017) and the broader confidence intervals on Kahn's index time series post-2003, suggest that recent trends in this index should be interpreted with caution.

DFA provides a useful tool to supplement the GLMM trend analyses. DFA was used to synthesize dozens of independent European Eel (*Anguilla anguilla*) time series into a common trend (ICES 2022) and was recommended for use by the review panel in the recent American

Eel stock assessment in the United States (ASMFC 2023). The conclusions drawn from the DFA results are largely consistent with the GLMM trend analysis. Long term declines were observed, primarily prior to the year 2000 with greater stability since. The DFA analysis also indicated potential periodic fluctuations, which may need further investigation, and could possible be related to climatic or oceanic conditions. However, with greater model fit issues and potential non-normality of the data, the DFA analysis should be interpreted with caution and used primarily to as a complement to the GLMM trend analysis.

The collection of datasets included in this analysis was subject to availability leading to an unbalanced model with datasets that vary in quality. The number of datasets representing the different zones was uneven, which could bias the Canada-wide trend estimate towards zones with the greatest representation. The inclusion of zone as a random intercept induces a correlation among observations within a zone, which should reduce the bias towards the zones with more datasets. The estimated standard deviations associated with zone, however, were generally small and highly uncertain (Tables A5.1 – A5.6), indicating that the correlation within zone was not that significant. Other approaches, such as weighting and sample analysis, were also used to investigate this bias. The overall conclusions were robust to these altered fits when the longer time series were retained.

The datasets included in the analysis varied in quality and consistency. Many of the datasets included were from surveys that do not target American Eel and instead capture them incidentally while targeting other species, such as Atlantic Salmon. When a species is not the target of the sampling effort there is an increased chance the species may be missed or not correctly enumerated. As well, American Eel propensity for burrowing (Tomie et al. 2017) may make them less susceptible to detection. In addition, there were changes to some sampling protocols that could not be controlled for through standardization. For example, the Saunders eel ladder dataset consists of counts of eels ascending the eel ladder on the Saunders side of the dam and in latter years the Moses side as well. Throughout the sampling period there have been changes to the ladder itself, changes to the methods used to count eel, and construction of an additional ladder on the American side of the dam (Cairns 2020). Any of these factors could contribute to variation in eel count not accounted for through standardization. For the East River elver trap dataset, there have been changes to how and how frequently calibration estimates were made to convert volumetric or weight measurements to elver counts (Bradford et al. 2022). The increase in calibration events likely lead to more accurate count estimates, which may contribute to the increase in elver counts in the latter years of the time series. In the St. Nicolas trap dataset, counts of numerous species were memorized before being recorded for a large portion of the time series, potentially leading to errors (Cairns 2020).

While it was the goal of this analysis to produce a Canada-wide trend in the relative abundance of American Eel through time, due to data availability, a better depiction of the results is a Canada-wide trend in American Eel relative abundance in freshwater where data were available. While this result is still useful and provides the best representation the status of American Eel in Canada, given the available data, there are a number of important caveats. A significant portion of the population may occupy marine or estuarine environments (Jessop et al. 2008) which were not represented in any of the time series analysed. In addition, there was only one dataset available from the Northern Gulf zone, which was located in New Brunswick, south of the St. Lawrence River, and there was no representation of the Labrador zone. This omits a significant portion of the freshwater habitat in Canada (Cairns et al. 2014). The temporal trend in abundance from marine, estuarine, and freshwater habitat north of the St. Lawrence River is not known and requires investigation to fully understand American Eel in Canada. As well, there was only one time series representing the elver or silver life stages. As such a depiction of the

state of these life-stages in Canada is not possible at present. This analysis grouping these stages with yellow eel which may be problematic.

Because sampling gear and protocols differed significantly among datasets it was not possible to assess American Eel density or total abundance among and within zones. Achievable densities may vary among zones which will impact the relative contribution of each zone to the total abundance of American Eel in Canada. Zones were either treated equally or weighted by total watershed area in the analyses applied. This may not accurately represent the historical or current distribution of American Eel within Canada. For example, the distribution of leptocephali to coastal areas of North America can be significantly affected by variation in the Gulf Stream, which could vary the relative number of eel distributed across the North American coastline (Rypina et al. 2016). Zone-specific densities driven by factors such as this would not be effectively represented by the modelling approach applied in this analysis.

To remedy the limitations of this Canada-wide trend analysis, standardized monitoring would need to be put in place. Consistent sampling methods or the ability to correct different methods by detection probability would allow for a comparison of density and, potentially, abundance across locations and zones. This would provide a much clearer picture of temporal changes and would not require standardization models and data-scaling transformations. Without standardized monitoring, an amalgamation of scaled abundance indices is the only reasonable approach to produce such a trend but there remain significant uncertainties related to data quality and appropriate weighting.

This analysis has not addressed the status or trajectory of American Eel outside of Canada. Canada represents only a portion of the habitat available to American Eel (Figure 1). As a single panmictic breeding population it is unlikely the Canadian population is independent of other jurisdictions. Extending the trend analysis to the full distribution of American Eel would be beneficial, and there are many fishery-independent time series from along the US Atlantic coast that could contribute to such an effort (ASMFC 2017). However, the addition of more datasets would not resolve the issues encountered in the present analysis.

REFERENCES

ASSG 2014. Anguilla rostrata. The IUCN Red List of Threatened Species. Version 2022-2.

ASMFC (Atlantic States Marine Fisheries Commission). 2017. 2017 American Eel Stock Assessment Update. Available: http://asmfc.org/fisheries-science/stock-assessments

ASMFC (Atlantic States Marine Fisheries Commission). 2023. American Eel benchmark stock assessment and peer review report. Available: http://asmfc.org/fisheries-science/stock-assessments.

Bowlby, H.D. 2018. Productivity of riverine habitat may be changing for American Eel. Can J. Fish. Aquat. Sci. 73: 1773-1777.

Bradford, R.G., Cook, A.M., and Smith, S. 2022. Assessment of the Maritimes Region American Eel and Elver fisheries. DFO Can. Sci. Advis. Sec. Res. Doc. 2022/009. v + 76 p.

Bowlby, H.D. 2018. Productivity of riverine habitats may be changing for American eel. Can. J. Fish. Aquat. Sci. 75: 1773-1777.

Cairns, D.K., Chaput, G.,Poirier, L.A.,Avery, T.S.,Castonguay, M.,Mathers, A., Casselman, J.M.,Bradford, R.G.,Pratt, T.,Verreault, G.,Clarke, K.,Veinott, G., and Bernatchez, L. 2014. Recovery Potential Assessment for the American Eel (Anguilla rostrata) for eastern Canada: life history, distribution, reported landings, status indicators, and demographic parameters. DFO Can. Sci. Advis. Sec. Res. Doc. 2013/134. xiv+157p.

Cairns, D.K. 2020. Landings, abundance indicators, and biological data for a potential range-wide American eel stock assessment. Can. Data Rep. Fish. Aquat. Sci. 1311: v + 180 p.

Cornic, M., Zhu X., Cairns D.K. 2021. Stock-wide Assessment Framework for American eel: Part 2-Review of trends and approaches to assessment. DFO Can. Sci. Advis. Sec. Res. Doc. 2021/032. vi + 71 p.

COSEWIC. 2012. COSEWIC assessment and status report on the American Eel *Anguilla rostrata* in Canada. Committee on the Status of Endangered Wildlife in Canada. Ottawa. xii + 109 pp. (www.registrelep-sararegistry.gc.ca/default_e.cfm).

DFO. 2014. Recovery potential assessment of American Eel (*Anguilla rostrata*) in eastern Canada. DFO Can. Sci. Advis. Sec. Sci. Advis. Rep. 2013/078. Hyperlink: http://www.dfo-mpo.gc.ca/csas-sccs/Publications/SAR-AS/2013/2013_078-eng.html.

Drouineau, H., Durif, C., Castonguay, M., Mateo, M., Rochard, E., Verrault, G., Yokouchi, K., and Lambert, P. 2018. Freshwater eels: a symbol of the effects of global change. Fish and Fisheries. 19: 903-930.

Greer, P.J. 2003. Distribution, relative abundance, and habitat use of American eel *Anguilla rostrata* in the Virginia portion of the Chesapeake Bay. Page 101-115 *in* D.A. Dixon, editor. Biology, management, and protection of catadromous eels. American Fisheries Society, Symposium 33, Bethesda, MD.

Haro, A., Richkus, W., Whalen, K., Hoar, A., Dieter Busch, W., Lary, S., Brush, T., and Dixon, D. 2000. Population decline of the American eel: implications for research and management. Fisheries. 25: 7-16.

Hartig, F. 2022. DHARMa: Residual diagnostics for hierarchical (multi-level/mixed) regression models. R package version 0.4.6, https://CRAN.R-project.org/package=DHARMa.

Holmes, E.E, Ward, E.J, Scheuerell, M,D., and Wills, K. 2024a. MARSS: Multivariate Autoregressive State-Space Modeling. R package version 3.11.9.

Holmes, E.E., Scheuerell, M.D., and Ward, E.J. 2024a. Analysis of multivariate time-series using the MARSS package. Version 3.11.9. NOAA Fisheries, Northwest Fisheries Science Center, 2725 Montlake Blvd E., Seattle, WA 98112, DOI: 10.5281/zenodo.5781847

ICES. 2022. Joint EIFAAC/ICES/GFCM Working Group on Eels (WGEEL).ICES Scientific Reports. 4:62. 297 pp. http://doi.org/10.17895/ices.pub.20418840

IUCN 2022. The IUCN Red List of Threatened Species. Version 2022-02. https://www.iucnredlist.org. Downloaded on 7/19/2023

Jacoby, D., Casselman, J., DeLucia, M. and Gollock, M. 2017. *Anguilla rostrata*. The IUCN Red List of Threatened Species 2017: e.T191108A121739077.

Jessop, B.M., Cairns, D.K., Thibault, I., and Tzeng, W.N. 2008. Life history of American eel Anguilla rostrata: new insights from otolith microchemistry. Aquat. Biol. 1: 205–216. doi:10.3354/ab00018.

Kahn, D.M. 2019. Trends in abundance and fishing mortality of American eels. Fisheries. 44: 129-136.

Landry-Massicotte, L.J., Dussureault, J., and Gamache, L. 2024. Estimation de l'abondance et caractérisation des anguilles d'Amérique (Anguilla rostrata) provenant des transferts dans la pêcherie commerciale de l'estuaire du Saint-Laurent en 2023. Ministère de l'Environnement, de la Lutte contre les changements climatiques, de la Faune et des Parcs, Direction de la gestion de la faune du Bas-Saint-Laurent. 17 p.

Rue, H., Martino, S., and Chopin, N. 2009. Approximate Bayesian inference for latent Gaussian models by using integrated nested Laplace approximations. J. R. Stat. Soc. Ser. B Stat. Methodol. 71(2): 319–392.

Rypina, I.I., Pratt, L.J., and Lozier, M.S. 2016. Influence of ocean circulation changes on the inter-annual variability of American eel larval dispersal. Limnol. Oceangr. 61: 1574-1588.

Simpson, D. Rue, H. Riebler, A. Nartins, T.G., and Sorbye, S.H. 2017. Penalising model component complexity: A principled, practical approach to constructing priors. Stat. Sci. 32: 1-28.

Sorbye, S.H., and Rue, H. 2017. Penalised complexity priors for stationary autoregressive processes. J. Time Ser. Anal. 38: 923-935.

Tomie, J.P.N, Cairns, D.K., Hobbs, R.S., Deshardins, M., Fletcher, G.L., and Courtenay, S.C. 2017. American eel (*Aguilla rostrata*) substrate selection for daytime refuge and winter thermal sanctuary. Mar. Freshw. Res. 68: 95-105. doi: 10.1071/MF15102.

Verreault, G., and P. Dumont. 2003. An estimation of American Eel escapement from the Upper St. Lawrence River and Lake Ontario in 1996 and 1997. Pages 243-251 in D.A. Dixon, editor. *Biology, Management, and Protection of Catadromous Eels*. American Fisheries Society Symposium. 33, Missouri.

Watanabe S. 2010. Asymptotic equivalence of Bayes cross validation and widely applicable information criterion in singular learning theory. J. Mach, Learn. 33: 3571-3594.

APPENDIX 1 – SCOTIA FUNDY STANDARDIZATION MODELS

Table A1.1. LaHave River standardization model fit statistic comparison across various random effects structures and probability distributions. The fits include the complete suites of potential fixed effect covariates. The selected model is indicated in bold. NB is negative binomial, ZIP is zero-inflated Poisson, ZINB is zero-inflated negative binomial. SSE is sum of squared estimates, KS is Kolmogorov-Smirnov, and WAIC is Watanabe-Akaike information criterion.

		Bayesian p-values				
Formula	Distribution	SSE	Residual Variance	# of Zeros	KS Test	WAIC
$y_{ist} \sim covariates + site_s + trib._t$	ZINB	0.999	0.938	0.454	0.052	1,376.5
$y_{is} \sim covariates + site_s$	ZINB	0.999	0.915	0.475	0.124	1,377.4
$y_{ist} \sim covariates + site_s + trib._t$	NB	1.000	0.986	0.875	0.028	1,404.1
$y_{is} \sim covariates + site_s$	NB	0.999	0.980	0.879	0.014	1,405.1
$\boldsymbol{y_{it} \sim covariates + trib._t}$	**ZINB**	**0.925**	**0.819**	**0.393**	**0.222**	**1,444.2**
$y_{it} \sim covariates + trib._t$	NB	0.955	0.881	0.742	0.516	1,450.7
$y_i \sim covariates$	NB	0.822	0.723	0.459	0.369	1,468.1
$y_i \sim covariates$	ZINB	0.882	0.795	0.726	0.342	1,468.5
$y_{ist} \sim covariates + site_s + trib._t$	Tweedie	0.658	0.255	1.000	0.400	1,479.5
$y_{it} \sim covariates + site_t$	Tweedie	0.676	0.282	1.000	0.218	1,481.5

Table A1.2. Nashwaak River standardization model fit statistic comparison across various random effects structures and probability distributions. The fits include the complete suites of potential fixed effect covariates. The selected model is indicated in bold. NB is negative binomial, ZIP is zero-inflated Poisson, ZINB is zero-inflated negative binomial. SSE is sum of squared estimates, KS is Kolmogorov-Smirnov, and WAIC is Watanabe-Akaike information criterion.

		Bayesian p-values				
Formula	Distribution	SSE	Residual Variance	# of Zeros	KS Test	WAIC
$\boldsymbol{y_{is} \sim covariates + site_s}$	**ZINB**	**0.976**	**0.756**	**0.618**	**0.356**	**2,719.0**
$y_i \sim covariates$	ZINB	0.788	0.526	0.714	0.443	2,744.7
$y_{is} \sim covariates + site_s$	Tweedie	0.875	0.631	1.000	0.449	2,784.5
$y_{is} \sim covariates + site_s$	NB	0.994	0.980	1.000	0.083	2,786.3
$y_i \sim covariates$	NB	0.969	0.944	1.000	0.098	2,790.3
$y_i \sim covariates$	Tweedie	0.470	0.180	1.000	0.355	2,799.4
$y_{is} \sim covariates + site_s$	ZIP	0.000	0.000	0.530	0.000	3,893.0
$y_{is} \sim covariates + site_s$	Poisson	0.000	0.000	1.000	0.000	4,325.7
$y_i \sim covariates$	ZIP	0.000	0.000	0.546	0.000	4,349.0
$y_i \sim covariates$	Poisson	0.000	0.000	1.000	0.000	5,293.8

Table A1.3. St. Mary's River standardization model fit statistic comparison across various random effects structures and probability distributions. The fits include the complete suites of potential fixed effect covariates. The selected model is indicated in bold. NB is negative binomial, ZIP is zero-inflated Poisson, ZINB is zero-inflated negative binomial. SSE is sum of squared estimates, KS is Kolmogorov-Smirnov, and WAIC is Watanabe-Akaike information criterion.

		Bayesian p-values				
Formula	Distribution	SSE	Residual Variance	# of Zeros	KS Test	WAIC
$y_{ist} \sim covariates + site_s + trib._t$	ZINB	0.986	0.260	0.158	0.245	2,135.5
$\boldsymbol{y_{is} \sim covariates + site_s}$	**ZINB**	**0.988**	**0.270**	**0.153**	**0.161**	**2,135.9**
$y_{ist} \sim covariates + site_s + trib._t$	NB	0.998	0.348	0.635	0.038	2,161.8
$y_{is} \sim covariates + site_s$	NB	0.999	0.370	0.658	0.023	2,162.6
$y_{it} \sim covariates + trib._t$	ZINB	0.944	0.335	0.182	0.270	2,174.7
$y_{it} \sim covariates + trib._t$	NB	0.980	0.403	0.607	0.058	2,194.1
$y_{ist} \sim covariates + site_s + trib._t$	Tweedie	0.891	0.015	0.970	0.115	2,224.6
$y_{is} \sim covariates + site_s$	Tweedie	0.875	0.026	0.965	0.087	2,224.7
$y_i \sim covariates$	ZINB	0.686	0.298	0.206	0.290	2,238.5
$y_i \sim covariates$	NB	0.847	0.348	0.624	0.116	2,250.1

Table A1.4. Chester River Elver Trap standardization model fit statistic comparison across various random effects structures and probability distributions. The fits include the complete suites of potential fixed effect covariates. The selected model is indicated in bold. NB is negative binomial, ZIP is zero-inflated Poisson, ZINB is zero-inflated negative binomial. SSE is sum of squared estimates, KS is Kolmogorov-Smirnov, and WAIC is Watanabe-Akaike information criterion.

		Bayesian p-values				
Formula	Distribution	SSE	Residual Variance	# of Zeros	KS Test	WAIC
$y_{iw} \sim covariates + week_{w,year}$	NB	1.000	1.000	1.000	0.000	20,989.2
$y_{iw} \sim covariates + week_{w,year}$	ZINB	1.000	0.761	0.952	0.000	21,004.7
$\boldsymbol{y_{im} \sim covariates + month_{m,year}}$	**ZINB**	**0.860**	**0.895**	**0.583**	**0.312**	**21,564.1**
$y_{id} \sim covariates + day_d$	ZINB	0.984	0.822	0.346	0.023	21,618.5
$y_{iw} \sim covariates + week_w$	ZINB	0.924	0.850	0.228	0.106	21,650.6
$y_{id} \sim covariates + day_d$	NB	0.996	0.906	1.000	0.000	21,692.4
$y_{iw} \sim covariates + week_w$	NB	0.986	0.886	0.998	0.001	21,716.7
$y_{im} \sim covariates + month_m$	ZINB	0.589	0.916	0.480	0.203	21,786.0
$y_i \sim covariates$	ZINB	0.486	0.888	0.222	0.171	21,788.9
$y_{im} \sim covariates + month_m$	NB	0.773	0.918	0.989	0.034	21,831.7

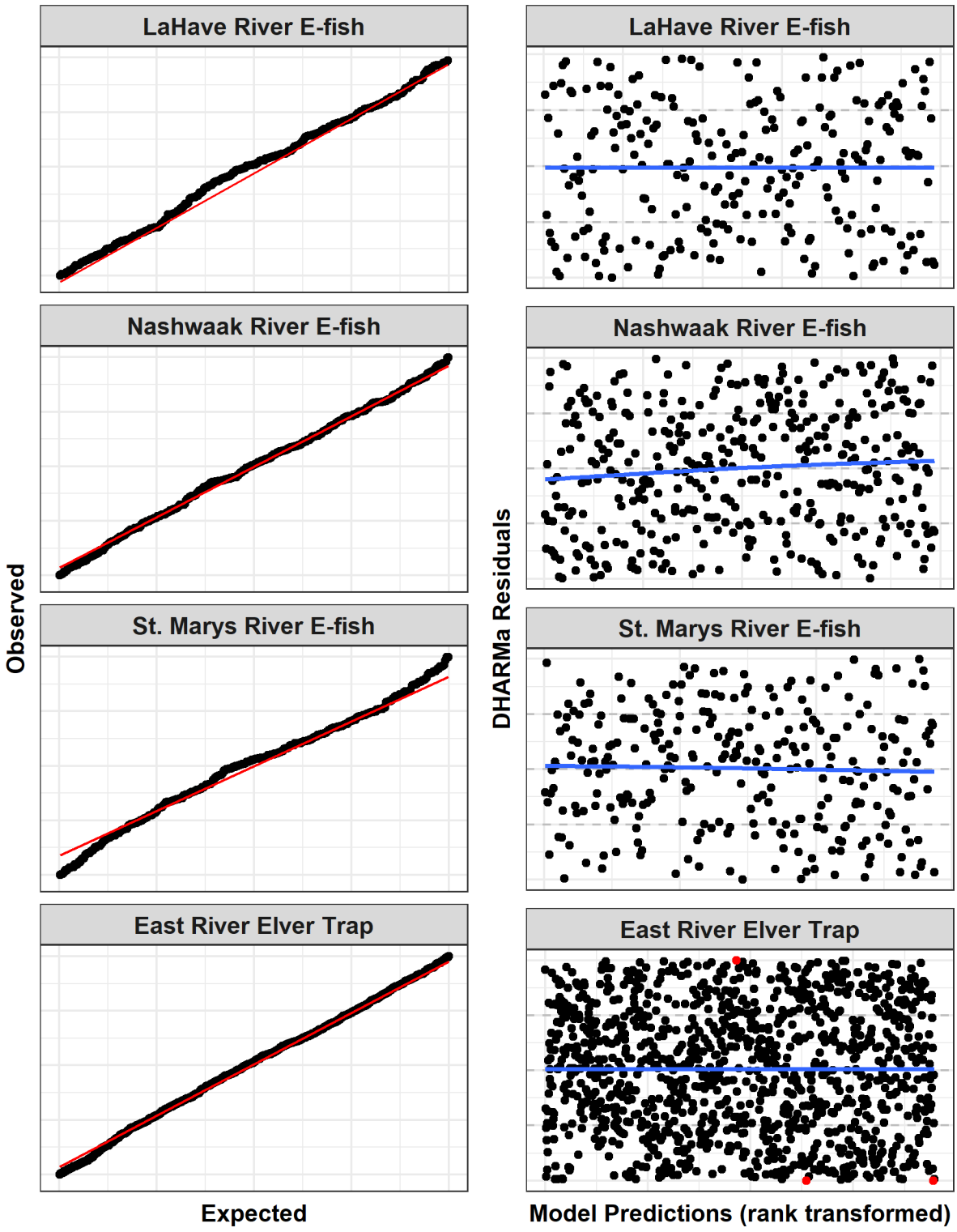

Figure A1.1. DHARMa residual plots for standardization models from datasets in the Scotia Fundy zone. Plots on the left are quantile-quantile plots comparing the distribution of the DHARMa residuals to a uniform distribution; the red line is a 1:1 reference line. The plots on the right are the DHARMa residuals plotted against the rank transformed model predictions; the blue line is a smoothed trend line and the red points represents potential outliers.

APPENDIX 2 – SOUTHERN GULF STANDARDIZATION MODELS

Table A2.1. Miramichi River standardization model fit statistic comparison across various random effects structures and probability distributions. The fits include the complete suites of potential fixed effect covariates. The selected model is indicated in bold. NB is negative binomial, ZIP is zero-inflated Poisson, ZINB is zero-inflated negative binomial. SSE is sum of squared estimates, KS is Kolmogorov-Smirnov, and WAIC is Watanabe-Akaike information criterion.

		Bayesian p-values				
Formula	Distribution	SSE	Residual Variance	# of Zeros	KS Test	WAIC
$\boldsymbol{y_{is} \sim covariates + site_s}$	**NB**	**0.998**	**0.987**	**0.827**	**0.057**	**7,852.1**
$y_{is} \sim covariates + site_s$	ZINB	0.998	0.980	0.820	0.069	7,853.8
$y_{is} \sim covariates + site_s$	Tweedie	0.662	0.000	1.000	0.000	7,981.4
$y_i \sim covariates$	NB	0.657	0.841	0.759	0.025	8,317.4
$y_i \sim covariates$	ZINB	0.675	0.807	0.754	0.025	8,319.4
$y_i \sim covariates$	Tweedie	0.000	0.000	1.000	0.000	8,660.7
$y_i \sim covariates$	ZIP	0.000	0.000	0.514	0.000	16,640.7
$y_{is} \sim covariates + site_s$	Poisson	0.000	0.000	1.000	0.000	21,033.3
$y_i \sim covariates$	Poisson	0.000	0.000	1.000	0.000	35,231.8

Table A2.2. Restigouche River standardization model fit statistic comparison across various random effects structures and probability distributions. The fits include the complete suites of potential fixed effect covariates. The selected model is indicated in bold. NB is negative binomial, ZIP is zero-inflated Poisson, ZINB is zero-inflated negative binomial. SSE is sum of squared estimates, KS is Kolmogorov-Smirnov, and WAIC is Watanabe-Akaike information criterion.

		Bayesian p-values				
Formula	Distribution	SSE	Residual Variance	# of Zeros	KS Test	WAIC
$y_{is} \sim covariates + site_s$	NB	0.998	1.000	0.927	0.116	2,742.7
$y_{is} \sim covariates + site_s$	ZINB	0.999	0.984	0.700	0.059	2,750.1
$\boldsymbol{y_{is} \sim covariates + site_s}$	**Tweedie**	**0.846**	**0.395**	**1.000**	**0.329**	**2,839.6**
$y_i \sim covariates$	ZINB	0.790	0.392	0.515	0.586	3,200.0
$y_i \sim covariates$	NB	0.784	0.472	0.858	0.747	3,239.9
$y_{is} \sim covariates + site_s$	ZIP	0.994	0.004	0.799	0.426	3,711.1
$y_i \sim covariates$	Tweedie	0.000	0.000	1.000	0.000	3,761.1
$y_i \sim covariates$	ZIP	0.001	0.001	0.473	0.084	6,076.4
$y_{is} \sim covariates + site_s$	Poisson	0.050	0.002	1.000	0.000	9,000.1
$y_i \sim covariates$	Poisson	0.000	0.000	1.000	0.000	32,175.6

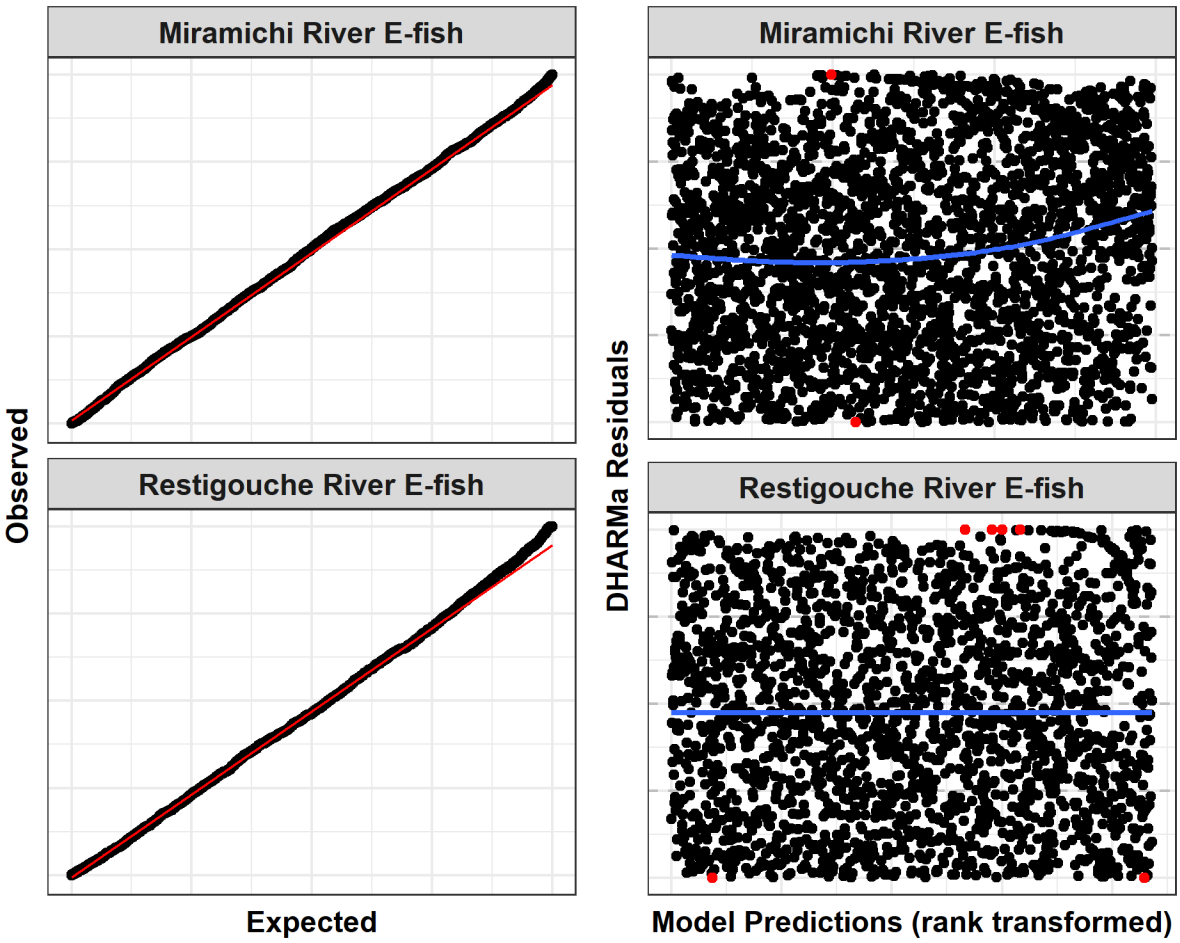

Figure A2.1. DHARMa residual plots for standardization models from datasets in the Southern Gulf zone. Plots on the left are quantile-quantile plots comparing the distribution of the DHARMa residuals to a uniform distribution; the red line is a 1:1 reference line. The plots on the right are the DHARMa residuals plotted against the rank transformed model predictions; the blue line is a smoothed trend line and the red points represents potential outliers.

APPENDIX 3 – NORTHERN GULF STANDARDIZATION MODELS

Table A3.1. Restigouche River standardization model fit statistic comparison across various random effects structures and probability distributions. The fits include the complete suites of potential fixed effect covariates. The selected model is indicated in bold. NB is negative binomial, ZIP is zero-inflated Poisson, ZINB is zero-inflated negative binomial. SSE is sum of squared estimates, KS is Kolmogorov-Smirnov, and WAIC is Watanabe-Akaike information criterion.

		Bayesian p-values				
Formula	Distribution	SSE	Residual Variance	# of Zeros	KS Test	WAIC
$y_{iw} \sim covariates + week_{w,year}$	ZINB	0.999	0.984	0.657	0.100	5,895.2
$y_{iw} \sim covariates + week_{w,year}$	NB	1.000	0.982	0.750	0.148	5,895.3
$\boldsymbol{y_{im} \sim covariates + month_{m,year}}$	**NB**	**0.654**	**0.800**	**0.686**	**0.515**	**6,122.5**
$y_{im} \sim covariates + month_{m,year}$	ZINB	0.661	0.776	0.657	0.440	6,124.1
$y_{id} \sim covariates + day_d$	NB	0.470	0.894	0.778	0.069	6,128.4
$y_{id} \sim covariates + day_d$	ZINB	0.466	0.881	0.724	0.069	6,129.0
$y_{iw} \sim covariates + week_w$	NB	0.376	0.886	0.770	0.135	6,135.6
$y_{iw} \sim covariates + week_w$	ZINB	0.324	0.869	0.750	0.130	6,137.3
$y_{im} \sim covariates + month_m$	NB	0.184	0.791	0.731	0.068	6,190.0
$y_{im} \sim covariates + month_m$	ZINB	0.172	0.772	0.702	0.012	6,192.0

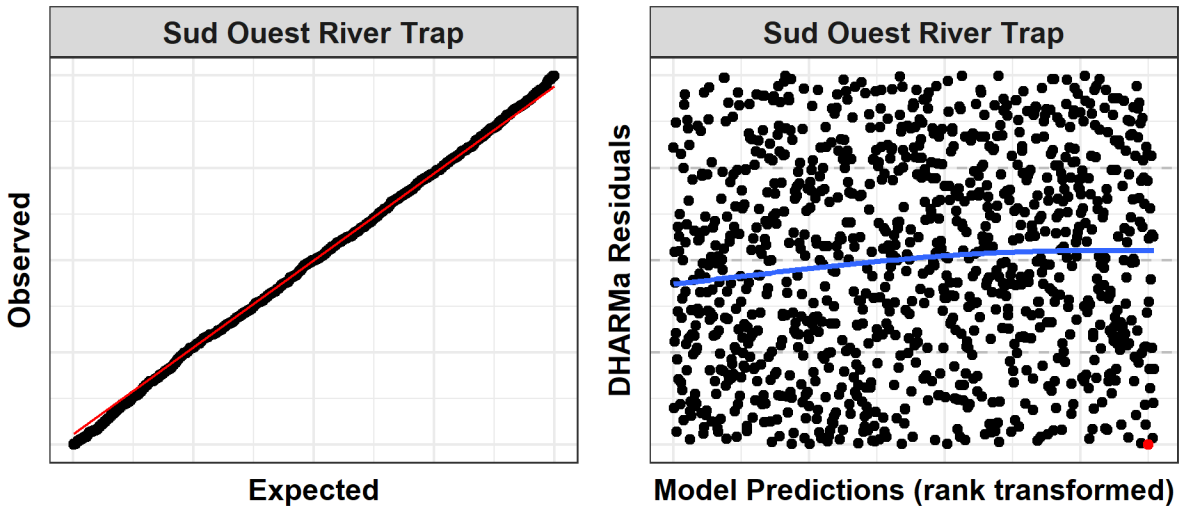

Figure A3.1. DHARMa residual plots for standardization models from the dataset in the Northern Gulf zone. Plot on the left are quantile-quantile plots comparing the distribution of the DHARMa residuals to a uniform distribution; the red line is a 1:1 reference line. The plot on the right are the DHARMa residuals plotted against the rank transformed model predictions; the blue line is a smoothed trend line and the red points represents potential outliers.

APPENDIX 4 – ST. LAWRENCE BASIN STANDARDIZATION MODELS

Table A4.1. Bay of Quinte standardization model fit statistic comparison across various random effects structures and probability distributions. The fits include the complete suites of potential fixed effect covariates. The selected model is indicated in bold. NB is negative binomial, ZIP is zero-inflated Poisson, ZINB is zero-inflated negative binomial. SSE is sum of squared estimates, KS is Kolmogorov-Smirnov, and WAIC is Watanabe-Akaike information criterion.

		Bayesian p-values				
Formula	Distribution	SSE	Residual Variance	# of Zeros	KS Test	WAIC
$y_{is} \sim covariates + site_s$	NB	0.897	0.875	0.602	0.804	2,439.6
$y_{is} \sim covariates + site_s$	ZINB	0.899	0.846	0.547	0.407	2,440.1
$\boldsymbol{y_i \sim covariates}$	**NB**	**0.894**	**0.868**	**0.627**	**0.486**	**2,441.0**
$y_i \sim covariates$	ZINB	0.884	0.833	0.549	0.448	2,441.9
$y_i \sim covariates$	Tweedie	0.618	0.028	0.958	0.758	2,563.2
$y_{is} \sim covariates + site_s$	Tweedie	0.635	0.035	0.947	0.540	2,563.5
$y_i \sim covariates$	ZIP	0.362	0.000	0.750	0.121	2,835.8
$y_{is} \sim covariates + site_s$	ZIP	0.360	0.000	0.738	0.004	2,840.0
$y_i \sim covariates$	Poisson	0.009	0.000	1.000	0.000	3,146.0
$y_{is} \sim covariates + site_s$	Poisson	0.010	0.000	1.000	0.000	3,185.7

Table A4.2. Saunders Dam eel ladder (1979 to 1995) standardization model fit statistic comparison across various random effects structures and probability distributions. The fits include the complete suites of potential fixed effect covariates. The selected model is indicated in bold. NB is negative binomial, ZIP is zero-inflated Poisson, ZINB is zero-inflated negative binomial. SSE is sum of squared estimates, KS is Kolmogorov-Smirnov, and WAIC is Watanabe-Akaike information criterion.

		Bayesian p-values				
Formula	Distribution	SSE	Residual Variance	# of Zeros	KS Test	WAIC
$y_{iw} \sim covariates + week_{w,year}$	ZINB	1.000	1.000	0.556	0.000	22,058.1
$y_{im} \sim covariates + month_{m,year}$	ZINB	1.000	1.000	0.548	0.000	22,925.8
$y_{id} \sim covariates + day_d$	ZINB	0.713	1.000	0.649	0.001	22,927.2
$\boldsymbol{y_{iw} \sim covariates + week_w}$	**ZINB**	**0.697**	**1.000**	**0.574**	**0.007**	**22,952.3**
$y_i \sim covariates$	ZINB	0.830	1.000	0.562	0.014	23,245.2
$y_{im} \sim covariates + month_m$	ZINB	0.820	1.000	0.561	0.005	23,245.3
$y_{iw} \sim covariates + week_{w,year}$	NB	1.000	1.000	1.000	0.000	23,876.5
$y_{id} \sim covariates + day_d$	NB	0.999	1.000	1.000	0.000	24,065.7
$y_{iw} \sim covariates + week_w$	NB	0.999	1.000	1.000	0.000	24,072.0
$y_{im} \sim covariates + month_{m,year}$	NB	1.000	1.000	1.000	0.000	24,117.6

Table A4.3. Saunders Dam eel ladder (2006 to 2018) standardization model fit statistic comparison across various random effects structures and probability distributions. The fits include the complete suites of potential fixed effect covariates. The selected model is indicated in bold. NB is negative binomial, ZIP is zero-inflated Poisson, ZINB is zero-inflated negative binomial. SSE is sum of squared estimates, KS is Kolmogorov-Smirnov, and WAIC is Watanabe-Akaike information criterion.

		Bayesian p-values				
Formula	Distribution	SSE	Residual Variance	# of Zeros	KS Test	WAIC
$y_{iw} \sim covariates + week_{w,year}$	NB	1.000	1.000	0.998	0.000	15,019.1
$y_{im} \sim covariates + month_{m,year}$	ZINB	1.000	1.000	0.940	0.005	16,052.8
$y_{im} \sim covariates + month_{m,year}$	NB	1.000	1.000	0.990	0.006	16,056.2
$y_{id} \sim covariates + day_d$	Tweedie	0.000	0.998	1.000	0.000	16,694.1
$y_{iw} \sim covariates + week_w$	Tweedie	0.000	0.999	1.000	0.000	16,730.5
$y_{id} \sim covariates + day_d$	ZINB	0.551	1.000	1.000	0.001	16,775.9
$\boldsymbol{y_{id} \sim covariates + day_d}$	**NB**	**0.552**	**1.000**	**1.000**	**0.001**	**16,776.5**
$y_{iw} \sim covariates + week_w$	ZINB	0.550	1.000	0.999	0.001	16,809.8
$y_{iw} \sim covariates + week_w$	NB	0.583	1.000	1.000	0.000	16,811.8
$y_{im} \sim covariates + month_m$	Tweedie	0.000	0.999	1.000	0.000	16,933.5

Table A4.4. Beauharnois Dam eel ladder standardization model fit statistic comparison across various random effects structures and probability distributions. The fits include the complete suites of potential fixed effect covariates. The selected model is indicated in bold. NB is negative binomial, ZIP is zero-inflated Poisson, ZINB is zero-inflated negative binomial. SSE is sum of squared estimates, KS is Kolmogorov-Smirnov, and WAIC is Watanabe-Akaike information criterion.

		Bayesian p-values				
Formula	Distribution	SSE	Residual Variance	# of Zeros	KS Test	WAIC
$y_{iw} \sim covariates + week_{w,year}$	Tweedie	1.000	1.000	1.000	0.000	21,105.5
$y_{iw} \sim covariates + week_{w,year}$	ZINB	1.000	1.000	0.483	0.000	21,158.4
$y_{iw} \sim covariates + week_{w,year}$	NB	1.000	1.000	1.000	0.000	21,521.1
$y_{im} \sim covariates + month_{m,year}$	ZINB	1.000	1.000	0.580	0.000	22,133.2
$y_{im} \sim covariates + month_{m,year}$	Tweedie	1.000	0.198	1.000	0.006	22,184.1
$\boldsymbol{y_{id} \sim covariates + day_d}$	**Tweedie**	**0.322**	**0.641**	**1.000**	**0.255**	**22,288.9**
$y_{im} \sim covariates + month_{m,year}$	NB	1.000	1.000	1.000	0.000	22,304.2
$y_{iw} \sim covariates + week_w$	Tweedie	0.300	0.604	1.000	0.382	22,335.6
$y_{id} \sim covariates + day_d$	ZINB	0.967	1.000	0.783	0.000	22,340.3
$y_{iw} \sim covariates + week_w$	ZINB	0.983	1.000	0.831	0.000	22,373.7

Table A4.5. Chambly Dam eel ladder standardization model fit statistic comparison across various random effects structures and probability distributions. The fits include the complete suites of potential fixed effect covariates. The selected model is indicated in bold. NB is negative binomial, ZIP is zero-inflated negative binomial, ZINB is zero-inflated negative binomial. SSE is sum of squared estimates, KS is Kolmogorov-Smirnov, and WAIC is Watanabe-Akaike information criterion.

		Bayesian p-values				
Formula	Distribution	SSE	Residual Variance	# of Zeros	KS Test	WAIC
$y_{iw} \sim covariates + week_{w,year}$	ZINB	1.000	0.416	0.003	0.003	8,296.5
$y_{iw} \sim covariates + week_{w,year}$	NB	1.000	0.509	0.018	0.000	8,359.4
$y_{im} \sim covariates + month_{m,year}$	ZINB	0.272	0.472	0.024	0.047	8,829.5
$\boldsymbol{y_{im} \sim covariates + month_{m,year}}$	**NB**	**0.404**	**0.476**	**0.028**	**0.072**	**8,834.5**
$y_{id} \sim covariates + day_d$	NB	0.022	0.714	0.042	0.076	8,976.8
$y_{id} \sim covariates + day_d$	ZINB	0.010	0.698	0.028	0.029	8,977.3
$y_{iw} \sim covariates + week_w$	ZINB	0.010	0.712	0.040	0.117	8,992.1
$y_{iw} \sim covariates + week_w$	NB	0.028	0.736	0.038	0.057	8,992.6
$y_i \sim covariates$	NB	0.000	0.752	0.056	0.018	9,155.0
$y_{im} \sim covariates + month_m$	NB	0.000	0.774	0.060	0.009	9,158.1

Table A4.6. St. Nicolas River standardization model fit statistic comparison across various random effects structures and probability distributions. The fits include the complete suites of potential fixed effect covariates. The selected model is indicated in bold. NB is negative binomial, ZIP is zero-inflated negative binomial, ZINB is zero-inflated negative binomial. SSE is sum of squared estimates, KS is Kolmogorov-Smirnov, and WAIC is Watanabe-Akaike information criterion.

		Bayesian p-values				
Formula	Distribution	SSE	Residual Variance	# of Zeros	KS Test	WAIC
$y_{iw} \sim covariates + week_{w,year}$	NB	1.000	0.080	0.299	0.071	14,509.0
$y_{iw} \sim covariates + week_{w,year}$	ZINB	1.000	0.082	0.323	0.100	14,510.7
$\boldsymbol{y_{id} \sim covariates + day_d}$	**NB**	**0.132**	**0.000**	**0.310**	**0.654**	**14,798.0**
$y_{id} \sim covariates + day_d$	ZINB	0.155	0.001	0.371	0.546	14,799.9
$y_{iw} \sim covariates + week_w$	NB	0.137	0.000	0.301	0.350	14,828.8
$y_{iw} \sim covariates + week_w$	ZINB	0.153	0.002	0.295	0.547	14,831.0
$y_{id} \sim covariates + day_d$	Tweedie	0.000	0.000	0.280	0.108	15,343.5
$y_{iw} \sim covariates + week_w$	Tweedie	0.000	0.000	0.319	0.034	15,382.2
$y_i \sim covariates$	NB	0.013	0.002	0.212	0.013	15,826.6
$y_{iw} \sim covariates$	ZINB	0.010	0.000	0.202	0.034	15,828.9

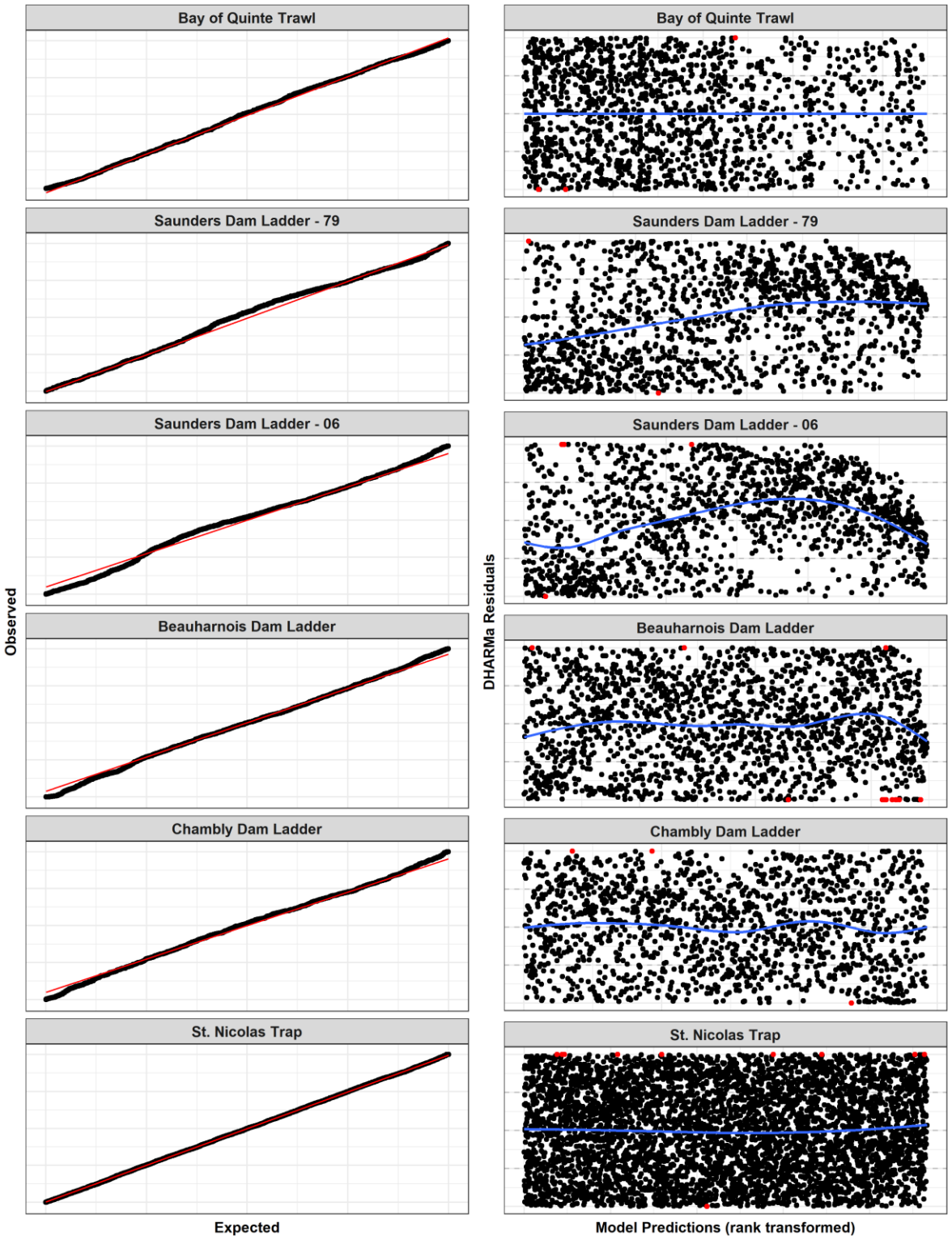

Figure A4.1. DHARMa residual plots for standardization models from datasets in the St. Lawrence Basin zone. Plots on the left are quantile-quantile plots comparing the distribution of the DHARMa residuals to a uniform distribution; the red line is a 1:1 reference line. The plots on the right are the DHARMa residuals plotted against the rank transformed model predictions; the blue line is a smoothed trend line and the red points represents potential outliers.

APPENDIX 5 – CANADA-WIDE TREND

Table A5.1. Canada-wide trend model parameter estimates fit to standardized abundance indices for all years of data. σ_y is the standard deviation of gaussian observations, κ is the shape parameter for gamma observations, $\sigma_{location}$ is the standard deviation for the dataset random intercept, $\sigma_{location,year}$ is the standard deviation for the random year slope by dataset, and σ_{zone} is the standard deviation for the zone random intercept.

	All Data Sets				Yellow Data Sets			
Parameters	**Mean**	**SD**	**LCI**	**UCI**	**Mean**	**SD**	**LCI**	**UCI**
Log_e-transformed								
Fixed Effects								
Intercept	1.835	1.162	-0.531	4.095	1.241	1.237	-1.278	3.663
Year	-0.034	0.006	-0.045	-0.023	-0.046	0.007	-0.059	-0.033
Hyperparameters								
σ_y	0.625	0.024	0.581	0.674	0.657	0.027	0.606	0.713
$\sigma_{location}$	3.266	0.61	2.259	4.646	2.635	0.641	1.646	4.148
$\sigma_{location,year}$	0.065	0.015	0.04	0.1	0.063	0.017	0.037	0.104
σ_{zone}	0.747	0.803	0.035	2.929	1.164	0.672	0.228	2.741
Scaled								
Fixed Effects								
Intercept	0.482	0.401	-0.368	1.257	0.44	0.475	-0.594	1.364
Year	-0.035	0.005	-0.044	-0.025	-0.042	0.005	-0.052	-0.032
Hyperparameters								
κ	0.588	0.021	0.547	0.631	0.615	0.024	0.57	0.664
$\sigma_{location}$	0.884	0.234	0.514	1.427	0.289	0.202	0.064	0.824
$\sigma_{location,year}$	0.058	0.014	0.036	0.089	0.06	0.016	0.036	0.097
σ_{zone}	0.363	0.352	0.033	1.317	0.814	0.407	0.291	1.853
Normalized								
Fixed Effects								
Intercept	-1.072	0.372	-1.882	-0.358	-1.067	0.452	-2.068	-0.194
Year	-0.036	0.005	-0.046	-0.026	-0.042	0.006	-0.053	-0.032
Hyperparameters								
κ	0.663	0.024	0.617	0.711	0.665	0.026	0.616	0.717
$\sigma_{location}$	0.729	0.239	0.367	1.295	0.402	0.275	0.096	1.131
$\sigma_{location,year}$	0.046	0.012	0.027	0.074	0.047	0.013	0.027	0.078
σ_{zone}	0.373	0.405	0.029	1.476	0.734	0.419	0.225	1.825

Table A5.2. Canada-wide trend model parameter estimates fit to standardized abundance indices for 1980-2018 years of data. σ_y is the standard deviation of gaussian observations, κ is the shape parameter for gamma observations, $\sigma_{location}$ is the standard deviation for the dataset random intercept, $\sigma_{location,year}$ is the standard deviation for the random year slope by dataset, and σ_{zone} is the standard deviation for the zone random intercept.

	All Data Sets				Yellow Data Sets			
Parameters	**Mean**	**SD**	**LCI**	**UCI**	**Mean**	**SD**	**LCI**	**UCI**
Log_e-transformed								
Fixed Effects								
Intercept	1.424	1.151	-0.897	3.681	0.708	1.162	-1.65	2.994
Year	-0.034	0.006	-0.046	-0.022	-0.046	0.007	-0.06	-0.032
Hyperparameters								
σ_y	0.658	0.027	0.608	0.715	0.694	0.031	0.635	0.758
$\sigma_{location}$	3.423	0.6	2.428	4.775	2.808	0.646	1.806	4.327
$\sigma_{location,year}$	0.067	0.016	0.041	0.103	0.066	0.018	0.039	0.109
σ_{zone}	0.708	0.879	0.027	3.105	0.883	0.704	0.081	2.676
Scaled								
Fixed Effects								
Intercept	0.207	0.402	-0.606	1.021	0.164	0.461	-0.771	1.103
Year	-0.032	0.006	-0.043	-0.021	-0.042	0.007	-0.055	-0.028
Hyperparameters								
κ	0.612	0.024	0.567	0.66	0.642	0.027	0.591	0.697
$\sigma_{location}$	0.954	0.213	0.621	1.454	0.798	0.24	0.436	1.371
$\sigma_{location,year}$	0.066	0.016	0.042	0.103	0.067	0.018	0.039	0.109
σ_{zone}	0.37	0.315	0.041	1.209	0.554	0.34	0.126	1.416
Normalized								
Fixed Effects								
Intercept	-1.347	0.323	-2.013	-0.696	-1.326	0.374	-2.094	-0.574
Year	-0.034	0.006	-0.046	-0.022	-0.044	0.008	-0.059	-0.029
Hyperparameters								
κ	0.71	0.027	0.659	0.765	0.718	0.03	0.662	0.779
$\sigma_{location}$	0.675	0.169	0.405	1.065	0.674	0.206	0.358	1.162
$\sigma_{location,year}$	0.059	0.015	0.035	0.092	0.057	0.017	0.032	0.097
σ_{zone}	0.321	0.285	0.035	1.084	0.391	0.305	0.056	1.196

Table A5.3. Canada-wide trend model parameter estimates fit to standardized abundance indices for 2000-2018 years of data. σ_y is the standard deviation of gaussian observations, κ is the shape parameter for gamma observations, $\sigma_{location}$ is the standard deviation for the dataset random intercept, $\sigma_{location,year}$ is the standard deviation for the random year slope by dataset, and σ_{zone} is the standard deviation for the zone random intercept.

	All Data Sets				Yellow Data Sets			
Parameters	**Mean**	**SD**	**LCI**	**UCI**	**Mean**	**SD**	**LCI**	**UCI**
Log_e-transformed								
Fixed Effects								
Intercept	1.085	1.187	-1.29	3.42	0.279	1.103	-1.945	2.454
Year	-0.014	0.008	-0.03	0.003	-0.017	0.009	-0.035	0.002
Hyperparameters								
σ_y	0.584	0.03	0.527	0.647	0.601	0.034	0.538	0.672
$\sigma_{location}$	3.606	0.617	2.571	4.987	3.004	0.593	2.058	4.375
$\sigma_{location,year}$	0.034	0.012	0.016	0.063	0.028	0.014	0.009	0.062
σ_{zone}	0.661	0.683	0.039	2.512	0.764	1.221	0.014	3.994
Scaled								
Fixed Effects								
Intercept	0.55	0.25	0.022	1.047	0.547	0.303	-0.093	1.161
Year	-0.013	0.008	-0.029	0.003	-0.017	0.009	-0.035	0
Hyperparameters								
κ	0.563	0.028	0.511	0.621	0.58	0.031	0.522	0.644
$\sigma_{location}$	0.486	0.123	0.293	0.772	0.3	0.112	0.139	0.573
$\sigma_{location,year}$	0.038	0.013	0.018	0.068	0.028	0.014	0.009	0.064
σ_{zone}	0.271	0.226	0.034	0.872	0.479	0.249	0.155	1.113
Normalized								
Fixed Effects								
Intercept	-1.114	0.203	-1.552	-0.708	-1.075	0.224	-1.556	-0.629
Year	-0.027	0.011	-0.048	-0.005	-0.027	0.012	-0.051	-0.003
Hyperparameters								
κ	0.775	0.037	0.705	0.851	0.797	0.041	0.72	0.88
$\sigma_{location}$	0.278	0.102	0.126	0.521	0.259	0.114	0.098	0.538
$\sigma_{location,year}$	0.053	0.018	0.026	0.096	0.028	0.016	0.007	0.069
σ_{zone}	0.242	0.202	0.031	0.779	0.286	0.212	0.047	0.841

Table A5.4. Canada-wide trend model parameter estimates fit to raw abundance indices for all years of data. σ_y is the standard deviation of gaussian observations, κ is the shape parameter for gamma observations, $\sigma_{location}$ is the standard deviation for the dataset random intercept, $\sigma_{location,year}$ is the standard deviation for the random year slope by dataset, and σ_{zone} is the standard deviation for the zone random intercept.

	All Data Sets				Yellow Data Sets			
Parameters	**Mean**	**SD**	**LCI**	**UCI**	**Mean**	**SD**	**LCI**	**UCI**
Log_e-transformed								
Fixed Effects								
Intercept	2.311	1.078	0.143	4.432	1.819	1.155	-0.518	4.098
Year	-0.029	0.007	-0.042	-0.015	-0.039	0.008	-0.055	-0.023
Hyperparameters								
σ_y	0.819	0.031	0.76	0.882	0.868	0.036	0.8	0.941
$\sigma_{location}$	3.123	0.568	2.172	4.398	2.578	0.644	1.59	4.102
$\sigma_{location,year}$	0.064	0.015	0.04	0.1	0.063	0.017	0.037	0.102
σ_{zone}	0.654	0.655	0.043	2.424	1.042	0.712	0.159	2.823
Scaled								
Fixed Effects								
Intercept	0.413	0.303	-0.207	1.03	0.379	0.347	-0.32	1.124
Year	-0.028	0.005	-0.039	-0.018	-0.032	0.006	-0.045	-0.021
Hyperparameters								
κ	0.779	0.027	0.728	0.834	0.821	0.031	0.763	0.883
$\sigma_{location}$	0.575	0.192	0.29	1.037	0.385	0.253	0.097	1.053
$\sigma_{location,year}$	0.054	0.013	0.034	0.084	0.059	0.015	0.036	0.094
σ_{zone}	0.291	0.287	0.028	1.069	0.488	0.32	0.12	1.332
Normalized								
Fixed Effects								
Intercept	-1.05	0.293	-1.647	-0.44	-1	0.355	-1.706	-0.248
Year	-0.024	0.005	-0.034	-0.014	-0.03	0.006	-0.042	-0.018
Hyperparameters								
κ	0.754	0.026	0.704	0.808	0.771	0.029	0.716	0.831
$\sigma_{location}$	0.457	0.206	0.168	0.964	0.423	0.254	0.122	1.088
$\sigma_{location,year}$	0.046	0.011	0.029	0.071	0.049	0.013	0.029	0.08
σ_{zone}	0.311	0.31	0.032	1.154	0.424	0.265	0.096	1.102

Table A5.5. Canada-wide trend model parameter estimates fit to raw abundance indices for 1980-2018 years of data. σ_y is the standard deviation of gaussian observations, κ is the shape parameter for gamma observations, $\sigma_{location}$ is the standard deviation for the dataset random intercept, $\sigma_{location,year}$ is the standard deviation for the random year slope by dataset, and σ_{zone} is the standard deviation for the zone random intercept.

	All Data Sets				Yellow Data Sets			
Parameters	**Mean**	**SD**	**LCI**	**UCI**	**Mean**	**SD**	**LCI**	**UCI**
Log_e-transformed								
Fixed Effects								
Intercept	1.948	1.056	-0.165	4.032	1.354	1.05	-0.762	3.431
Year	-0.027	0.007	-0.041	-0.012	-0.037	0.009	-0.054	-0.019
Hyperparameters								
σ_y	0.832	0.034	0.767	0.901	0.885	0.04	0.81	0.966
$\sigma_{location}$	3.209	0.561	2.255	4.453	2.637	0.584	1.715	3.998
$\sigma_{location,year}$	0.068	0.016	0.042	0.105	0.069	0.018	0.041	0.113
σ_{zone}	0.658	0.948	0.025	3.19	0.763	0.705	0.055	2.639
Scaled								
Fixed Effects								
Intercept	0.103	0.361	-0.615	0.843	0.053	0.424	-0.788	0.928
Year	-0.025	0.007	-0.039	-0.011	-0.033	0.009	-0.049	-0.015
Hyperparameters								
κ	0.808	0.03	0.751	0.868	0.857	0.035	0.791	0.927
$\sigma_{location}$	0.86	0.196	0.545	1.31	0.818	0.235	0.453	1.371
$\sigma_{location,year}$	0.064	0.015	0.04	0.1	0.068	0.018	0.04	0.11
σ_{zone}	0.334	0.327	0.033	1.22	0.428	0.314	0.067	1.244
Normalized								
Fixed Effects								
Intercept	-1.3	0.306	-1.91	-0.666	-1.295	0.359	-2.008	-0.552
Year	-0.021	0.007	-0.034	-0.009	-0.03	0.008	-0.045	-0.014
Hyperparameters								
κ	0.754	0.028	0.7	0.812	0.772	0.032	0.712	0.837
$\sigma_{location}$	0.682	0.168	0.413	1.07	0.732	0.208	0.413	1.223
$\sigma_{location,year}$	0.057	0.014	0.035	0.089	0.059	0.016	0.034	0.096
σ_{zone}	0.286	0.252	0.032	0.962	0.339	0.29	0.041	1.113

Table A5.6. Canada-wide trend model parameter estimates fit to raw abundance indices for 2000-2018 years of data. σ_y is the standard deviation of gaussian observations, κ is the shape parameter for gamma observations, $\sigma_{location}$ is the standard deviation for the dataset random intercept, $\sigma_{location,year}$ is the standard deviation for the random year slope by dataset, and σ_{zone} is the standard deviation for the zone random intercept.

	All Data Sets				Yellow Data Sets			
Parameters	**Mean**	**SD**	**LCI**	**UCI**	**Mean**	**SD**	**LCI**	**UCI**
Log_e-transformed								
Fixed Effects								
Intercept	1.835	1.162	-0.531	4.095	1.009	1.006	-1.001	3.005
Year	-0.034	0.006	-0.045	-0.023	-0.01	0.012	-0.033	0.014
Hyperparameters								
σ_y	0.625	0.024	0.581	0.674	0.766	0.043	0.685	0.855
$\sigma_{location}$	3.266	0.61	2.259	4.646	2.686	0.536	1.803	3.902
$\sigma_{location,year}$	0.065	0.015	0.04	0.1	0.035	0.016	0.012	0.073
σ_{zone}	0.747	0.803	0.035	2.929	0.631	0.588	0.046	2.199
Scaled								
Fixed Effects								
Intercept	1.687	1.078	-0.459	3.82	0.469	0.235	-0.023	0.947
Year	-0.01	0.01	-0.03	0.011	-0.009	0.015	-0.038	0.02
Hyperparameters								
κ	0.736	0.038	0.665	0.815	1.004	0.049	0.912	1.104
$\sigma_{location}$	0.353	0.116	0.173	0.625	0.348	0.136	0.146	0.673
$\sigma_{location,year}$	0.021	0.015	0.003	0.06	0.025	0.02	0.004	0.078
σ_{zone}	0.212	0.183	0.026	0.702	0.295	0.238	0.05	0.933
Normalized								
Fixed Effects								
Intercept	-0.977	0.13	-1.247	-0.711	-0.959	0.149	-1.268	-0.655
Year	-0.014	0.011	-0.035	0.008	-0.012	0.012	-0.036	0.013
Hyperparameters								
κ	0.796	0.038	0.725	0.872	0.817	0.041	0.739	0.901
$\sigma_{location}$	0.193	0.087	0.071	0.406	0.212	0.097	0.073	0.445
$\sigma_{location,year}$	0.039	0.017	0.015	0.081	0.025	0.016	0.005	0.064
σ_{zone}	0.143	0.128	0.018	0.488	0.162	0.149	0.018	0.566

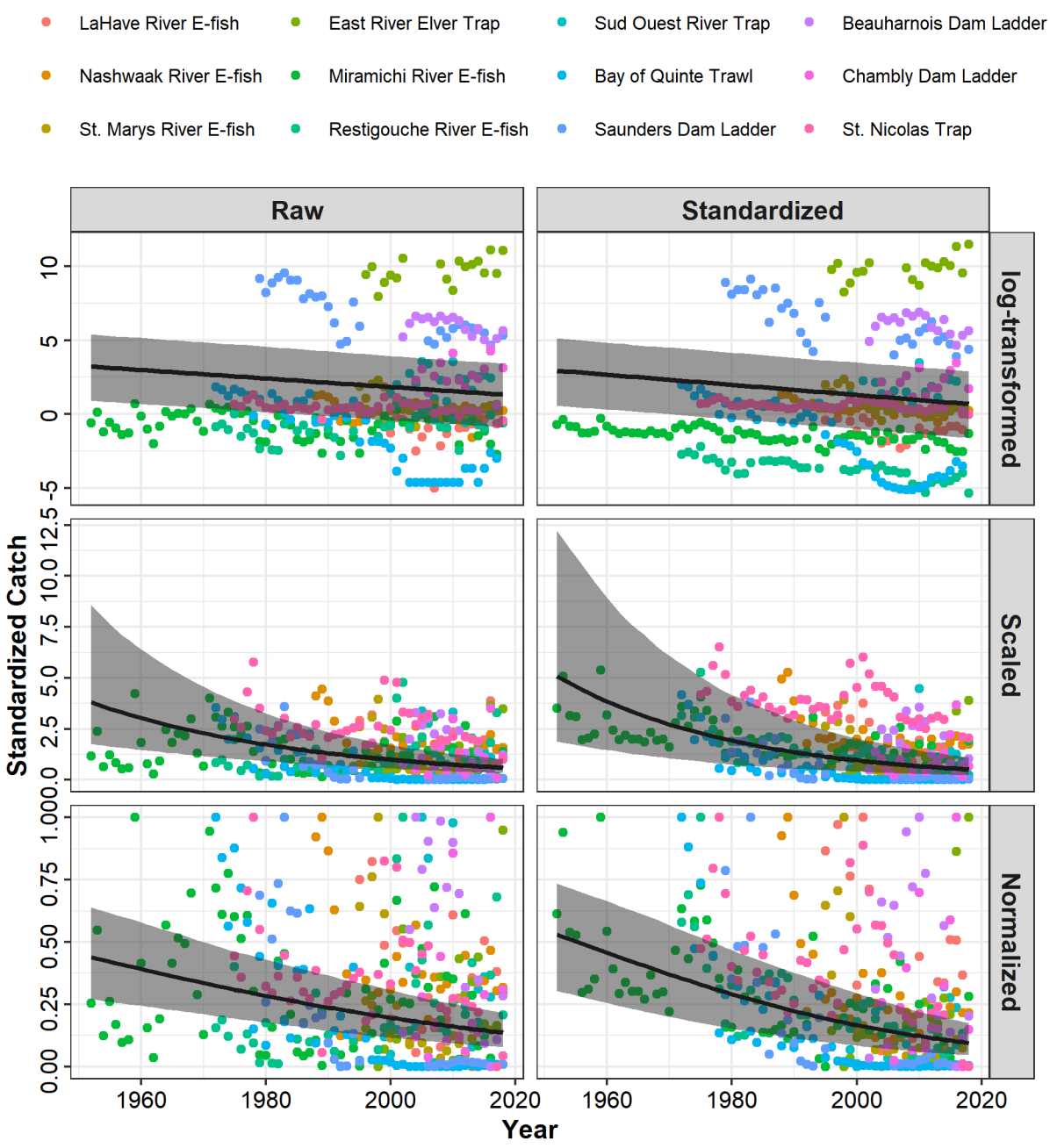

Figure A5.1. Canada-wide trend analysis results for models fit to raw and standardized indices of relative abundance from all years of data. Three transformation methods were used to scale the datasets. The black line indicates the mean trend and the grey area indicates 95% credible intervals.

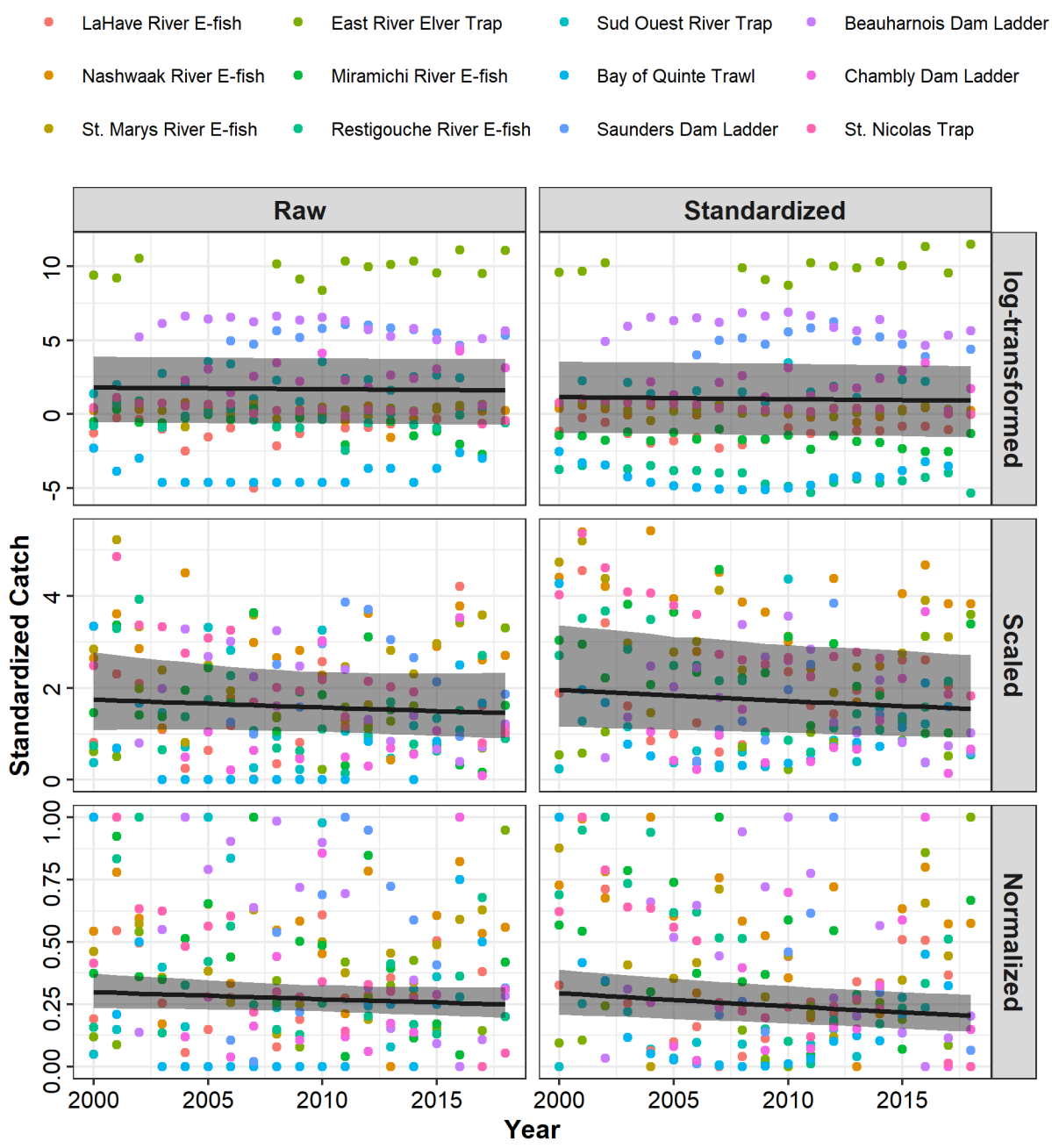

Figure A5.2. Canada-wide trend analysis results for models fit to raw and standardized indices of relative abundance from years 2000-2018. Three transformation methods were used to scale the datasets. The black line indicates the mean trend and the grey area indicates 95% credible intervals.

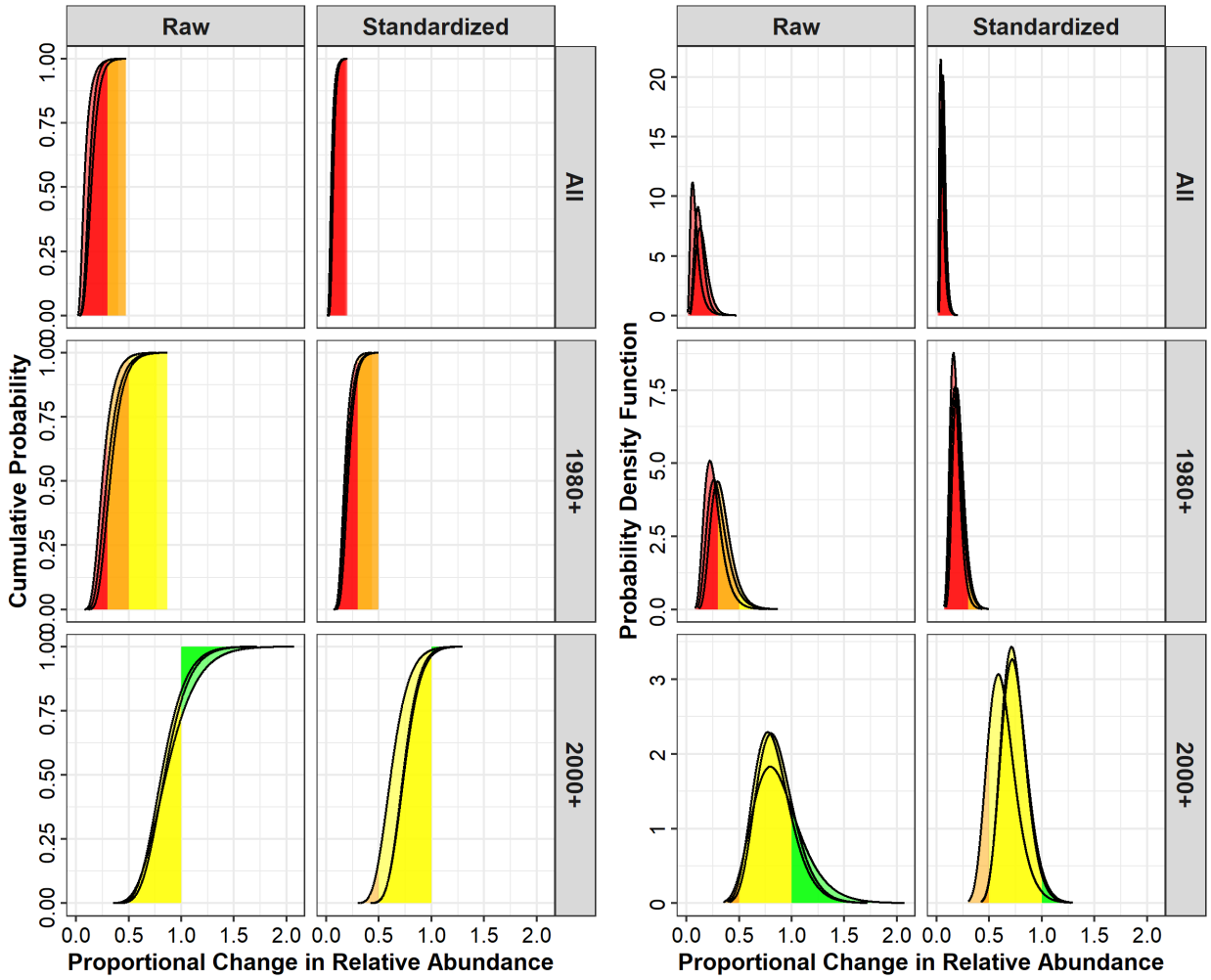

Figure A5.3. Cumulative probability (left) and probability density function (right) of levels of proportional population change for American Eel in Canada estimated for three temporal periods (All: 1952 to 2018; 1980+: 1980 to 2018; and 2000+: 2000 to 2018) for standardized and raw data using ten yellow stage America Eel data timeseries. The lines represents results for the three data transformation methods. Colours represents different levels of population change: red - > 70% decline, orange - 50-70% decline, yellow: decline < 50%, green: population increase.

APPENDIX 6 – DYNAMIC FACTOR ANALYSIS – RAW DATA

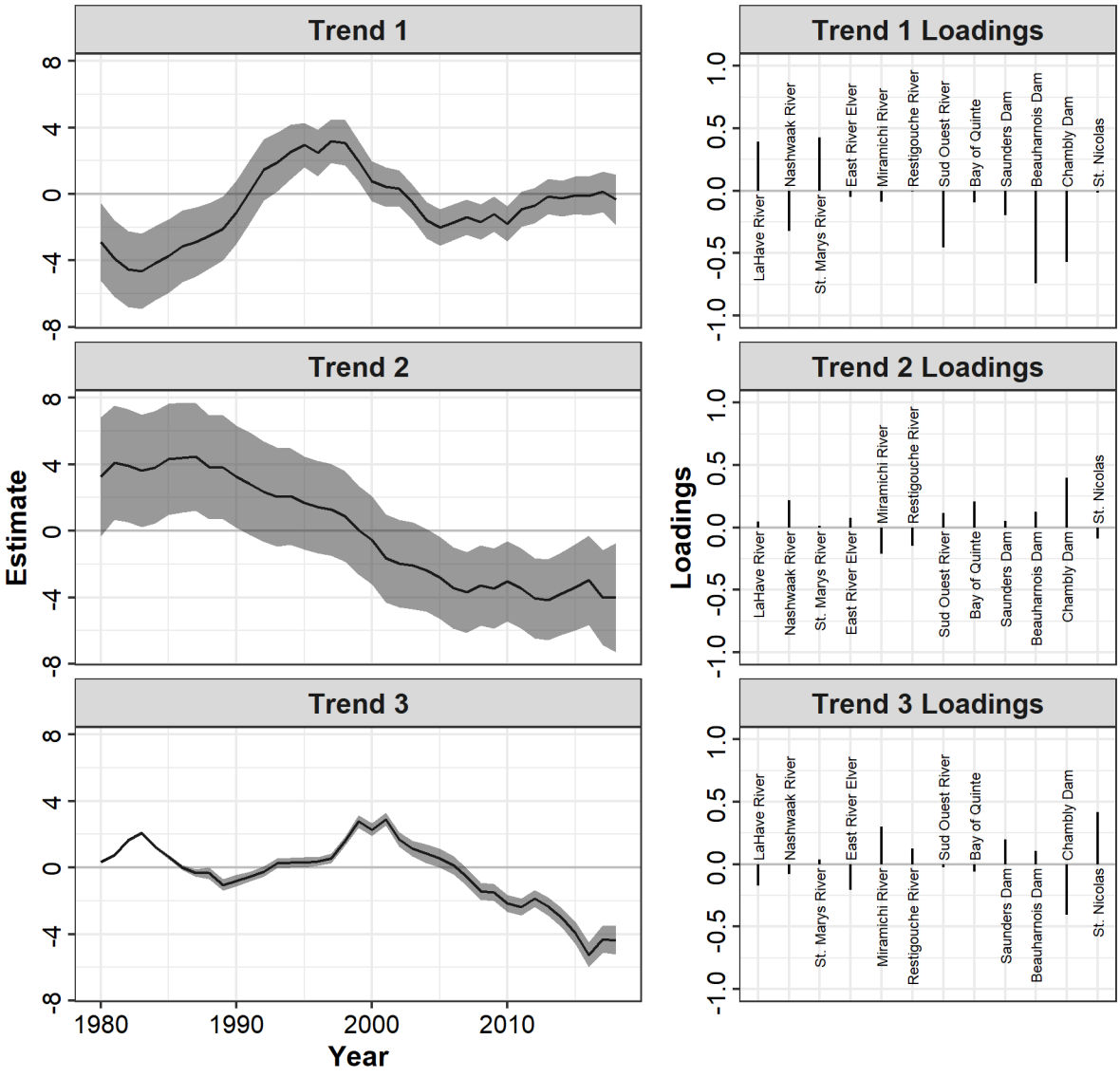

Figure A6.1. Dynamic factor analysis results fit to raw (unstandardized) data for years 1980-2018. The left column depicts the estimated trend lines and the right column depicts of the loading values associated with the trend line for each time series.

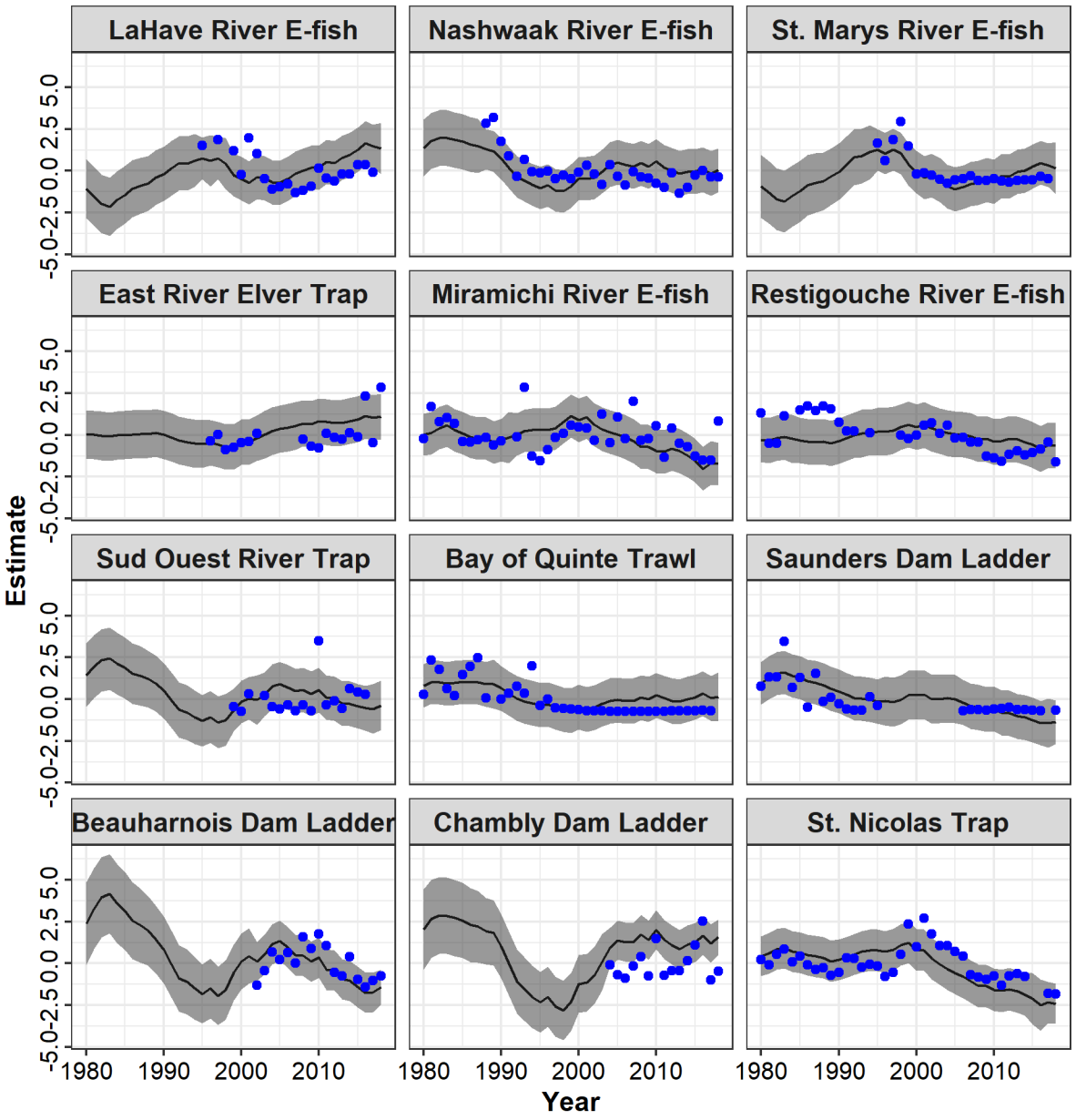

Figure A6.2. Time series-specific predictions from dynamic factor analysis fit to raw (unstandardized) data for years 1980-2018. The blue points are the data, the black line is the mean predictions and the grey area is the confidence intervals.